Ecological Processes

RESEARCH

Open Access

Ecological niche modelling of a critically endangered species *Commiphora wightii* (Arn.) Bhandari using bioclimatic and non-bioclimatic variables

Manish Mathur[1*], Preet Mathur[2] and Harshit Purohit[3]

Abstract

Background The aim of this study is to examine the effects of four different bioclimatic predictors (current, 2050, 2070, and 2090 under Shared Socioeconomic Pathways SSP2-4.5) and non-bioclimatic variables (soil, habitat heterogeneity index, land use, slope, and aspect) on the habitat suitability and niche dimensions of the critically endangered plant species *Commiphora wightii* in India. We also evaluate how niche modelling affects its extent of occurrence (EOO) and area of occupancy (AOO).

Results The area under the receiver operating curve (AUC) values produced by the maximum entropy (Maxent) under various bioclimatic time frames were more than 0.94, indicating excellent model accuracy. Non-bioclimatic characteristics, with the exception of terrain slope and aspect, decreased the accuracy of our model. Additionally, Maxent accuracy was the lowest across all combinations of bioclimatic and non-bioclimatic variables (AUC = 0.75 to 0.78). With current, 2050, and 2070 bioclimatic projections, our modelling revealed the significance of water availability parameters (BC-12 to BC-19, i.e. annual and seasonal precipitation as well as precipitation of wettest, driest, and coldest months and quarters) on habitat suitability for this species. However, with 2090 projection, energy variables such as mean temperature of wettest quarter (BC-8) and isothermality (BC-3) were identified as governing factors. Excessive salt, rooting conditions, land use type (grassland), characteristics of the plant community, and slope were also noticed to have an impact on this species. Through distribution modelling of this species in both its native (western India) and exotic (North-east, Central Part of India, as well as northern and eastern Ghat) habitats, we were also able to simulate both its fundamental niche and its realized niche. Our EOO and AOO analysis reflects the possibility of many new areas in India where this species can be planted and grown.

Conclusion According to the calculated area under the various suitability classes, we can conclude that *C. wightii*'s potentially suitable bioclimatic distribution under the optimum and moderate classes would increase under all future bioclimatic scenarios (2090 > 2050 ≈ current), with the exception of 2070, demonstrating that there are more suitable habitats available for *C. wightii* artificial cultivation and will be available for future bioclimatic projections of 2050 and 2090. Predictive sites indicated that this species also favours various types of landforms outside rocky environments, such as sand dunes, sandy plains, young alluvial plains, saline areas, and so on. Our research also revealed crucial information regarding the community dispersion variable, notably the coefficient of variation that, when bioclimatic + non-bioclimatic variables were coupled, disguised the effects of bioclimatic factors across all time frames.

*Correspondence:
Manish Mathur
eco5320@gmail.com
Full list of author information is available at the end of the article

Keywords *Commiphora wightii*, Critically endangered, Maxent, Habitat heterogeneity index, Niche hypervolume, Area of extent, Area of occupancy

Introduction

Evidence from the literature suggests that climate change is happening now and has a direct effect on biodiversity, forcing species to adapt either through migrating, changing phenological cycles, or developing new physiological traits (Behera and Roy 2019). As per the Millennium Ecosystem Assessment (2005), climate change is likely to become one of the most substantial drivers of biodiversity loss by the end of the present century. Climate change is imposing severe threats to, and having dramatic effects on, a wide range of India's plants and animals (Ray et al. 2014). India is both a major greenhouse gas emitter and one of the most vulnerable countries in the world to projected climate change. The country is already experiencing changes in climate and the impacts of climate change, including water stress, heat waves and drought, severe storms and flooding, and associated negative consequences on health and livelihoods. With a 1.2 billion populations and dependence on agriculture, India probably will be severely impacted by continuing climate change. Global climate projections, given inherent uncertainties, indicate several changes in India's future climate. Even with a conservative temperature increase of 1 to 2 °C, most ecosystems and landscapes will be impacted through changes in species composition, productivity and biodiversity. Impacts to the country as a whole are also projected by way of economically important forest types, such as *Tectona grandis, Shorea robusta*, bamboo, upland hardwoods and pine (Behera et al. 2019).

Human-caused accelerated climate change has now been added to the natural variability, threatening to exacerbate the loss of biodiversity already underway as a result of other human stressors. As a result, there is an urgent need to collect and disseminate information in order to contribute to the development of a strategic plan for climate change mitigation and adaptation. Modelling a species' ecological niche and potential distribution of economically valuable and Rare Endangered and Threatened (RET) plant species under projected climate change impacts may help us understand their behaviour under altered climatic conditions.

The ecological niche model (ENM) is a statistical approximation regarding distribution of a species as well as it links their location data to environment variables by using statistical techniques in order to describe, understand, and/or predict the distribution of species (Sillero et al. 2021). ENM's mathematical outputs can be either an equation that relates a species' predicted distribution to a set of environmental predictors, or a response curve that explains how the predictors control species distribution. Further, mathematical model can be specialized into a cartographic model, i.e. a map showing habitat suitability, probability of species occurrence, or the favorability for species occurrence. Therefore, ENMs are forecast in the environmental space and projected into the geographical space. Various disciplines, such as global change biology, biogeography, and conservation management, have adopted ENM (Mathur and Mathur 2023).

With presence–absence data, there are two subgroups for ENM: regression-based and machine learning. Generalized linear models (GLM), generalized additive models (GAM), and multivariate adaptive regression splines (MARS) are examples of regression-based techniques. Artificial neural network (ANN), classification trees (CART), maximum entropy (Maxent), genetic algorithm (GARP), and random forest (RF) are examples of machine learning algorithms. Pecchi et al. (2019) describe these techniques in detail. In summary, these methods differ in terms of species records (absence/presence or presence-only) and the parameters used to make predictions (mechanistic-physiological constraint or empirical-climatic approach).

Maxent, for example, has grown in popularity since its debut (Renner and Warton 2013). Maxent estimates a target probability distribution by calculating the probability distribution of maximum entropy (Phillips et al. 2006), making it highly applicable to species distribution modelling (Wang et al. 2015). Maxent can also project shifts in species distributions under different climate change scenarios, with topography, soil characteristics, land use, and biological interactions identified as the main determinants of species distributions at different geographical scales (Abolmaali et al. 2017). Meanwhile, as a presence-only model, Maxent compares the distribution of presences along environmental gradients to the distribution of background points drawn at random from the study area using a background sample (Vitor et al. 2018). In general, Maxent (Phillips et al. 2006) is a promising method for modelling rare species for several reasons: (1) the results are robust at sample sizes as small as 10; (2) it consistently outperforms other predictive modelling methods in discrimination success (Wisz et al. 2008); (3) it can incorporate categorical environmental data, such as soils and geology; and (4) it is a presence-only method

that does not require the identification of absence locations. Maxent generates a continuous output of habitat suitability values ranging from 0 to 1, with 0 being the least suitable and 1 being the most suitable. This software generates robust models if more than 30 occurrence points for each species are available (Elith et al. 2011). Globally, researchers have looked into the efficient use of the maxent tool for ecological niche modelling of Rare Endangered and Threatened (RET) plant species (Buechling and Tobalske 2010; Gogol-Prokurat 2011; De Queiroz et al. 2012; Wang et al. 2015; Cihal and Kalab 2017; Salam et al. 2018; McCune et al. 2020 and Rahaman et al. 2022). These inquests concentrated on plant species belonging to the gymnosperm, angiosperm, pteridophytes, bryophytes, orchids, fungi, and bacteria groups.

The genus *Commiphora* Jacq. (Burseraceae) contains approximately 185 species that are found in tropical areas ranging from Africa to Madagascar, Asia, Australia, and the Pacific Islands (Barve and Mehta 1993; Kumar and Shanker 1982; Lal and Kasera 2010 and Reddy et al. 2012). *C. wightii, C. agallocha*, and *C. berryi* are native to India (Lal and Kasera 2010 and Ramawat et al. 2008).

For *Commiphora wightii*, reproductive isolation, combined with the dominance of apomictic behaviour (asexual mode of reproduction), may have a negative impact on genetic variation. Because of the high level of population differentiation, the population continuum has been disrupted, possibly as a result of overexploitation, unsustainable exploitation, and other anthropogenic activities (Reddy et al. 2012). Furthermore, climatic conditions, soil erosion, low rainfall, termite infestation, domestic animal overgrazing, and mining activities have all had an impact on existing natural populations of this species (Haque et al. 2009). These prevalent abiotic factors, combined with mass destruction, poor regeneration, and non-survival due to poor tapping methods, have resulted in a significant setback for plant stands in natural habitats (Kulloli et al. 2016). *C. wightii* was classified as vulnerable in 1998 and critically endangered (CR) on The IUCN Red List of Threatened Species under criteria A2cd in 2014, based on the cumulative effects of these factors and the current rate of decline in populations in their native habitats (Ved et al. 2015).

Apart from acknowledging its economic value and extinction risks, empirical evidence is required to predict the effects of current and future bioclimatic phenomena, as well as other geomorphological attributes, on its habitat suitability as well as for its current and projected area of occupancy on a larger geographical scale. As a result, the current study was designed to answer the following questions: (a) What is the relationship between this species' geographical distribution and current bioclimatic variables, as well as other factors like soil, slope, land use, and habitat heterogeneity (i.e. plant community attributes)? (b) How will this species react to future bioclimate scenarios? (c) How will the interaction of all of these bioclimatic and non-bioclimatic variables affect its habitat suitability? (d) How do the species' extent of occurrence (EOO) and area of occupancy (AOO) relate to its current and projected geographical distribution?

Materials and methods

Study species

Commiphora wightii (Arn.) Bhandari is a deciduous species also known as "guggal" and "Indian Bdellium" that can grow either erect (Fig. 1A) or spread (Fig. 1B) and such branching patterns are valuable morphological differentiation among female and male plants along with other morphological traits like bark types, leaf and spine morphology and petiole architecture (Holscher 2011; Kulhari et al. 2014; Gaur et al. 2017). Because female plants tend to outnumber male plants in nature (Gupta et al. 1996), there is less pollen accessible for fertilization. Seed germination is stymied by the seed's stiff endocarp, which blocks the entry of water, impairs gas exchange, and stunts embryo development. The poor germination rate of 1.4% can be attributed to the challenging natural conditions (Yadav et al. 1999).

Rajasthan has largest area covering guggal population but density is still very poor. Highest density of guggal is reported in Sawai Madhopur ($\approx$74 plants ha^{-1} Fig. 1C) and Jhunjhunu ($\approx$69 plants ha^{-1}) districts of Rajasthan (Tomar 2021). It has been designated as a priority species for research and development by the National Medicinal Plant Board, Ministry of Ayush, New Delhi (Kala et al 2006). Oleo-gum resin is extracted from the bark of this plant and has powerful medicinal properties, particularly in the treatment of arthritis, bronchitis, cholesterol reduction, hyperlipidaemia, atherosclerosis, and coronary artery disease (Wu et al. 2002).

Rural residents are aware of its market value and thus collect the gum resin by making unscientific cuts in the stem (Fig. 1D). In recent years, they have begun to apply copper sulphate to the cuts in order to increase yield, which may be harmful to the plant (Fig. 1E; Singh and Singh 2006). Due to destructive harvesting practices and population reduction, the trend of guggul gum collection has declined rapidly in recent years. In Gujarat, a key production area, gum resin collection was 30 tons in 1963, but it was reduced to 2.42 tons in 1999 (Dixit and Rao 2000). The actual demand for guggul gum in India is around 1000 tons per year, but production is only 100 tons. The deficit is filled through imports from the Pakistan and Afghanistan, for which India pays approximately 45 crore rupees per year (Maheshwari 2010).

Fig. 1 *C. wightii* species. Erect habit (**A**); spread/bushy habit deciduous in nature (**B**); plantation for germplasm conservation (**C**); non-woody stem: source of oleo-gum resin (**D**) and non-scientific tapping for gum extraction lead plant death (**E**)

Observations revealed that this species is threatened throughout its entire range in Rajasthan and Gujarat (Bishoni et al. 2018). It is estimated that within a decade or so, the population as a whole has shrunk to less than 50%, with scattered and dissected subpopulations of few mature individuals in each (Parmar 2003; Jain and Nadgauda 2013). According to Reddy et al. (2012), *C. wightii* is facing severe conservation threats and extinction risk due to overexploitation, narrow range of occurrence, small area of occupancy, severe fragmentation of populations, very low regeneration, and invasion of alien species into its habitat.

Species distribution

Distributional records for this species were obtained from data repositories such as the Global Biodiversity Information Facility (www.gbif.org/), Indian Biodiversity Portal (https://indiabiodiversity.org/species/show/33318), and published literature (Dixit and Rao 2000; Reddy et al. 2012; Harish et al. 2014; Kulhari et al. 2014; Bishoni et al. 2018; Saini et al. 2018; Mathur and Sundaramoorthy 2019; Choudhary et al. 2021; Verma et al. 2022) as well as from our field survey at Sirohi district of Rajasthan (Jindal et al. 2009, 2010). Using high-resolution Google Earth satellite image data and GIS ArcMap (Coban et al. 2020) software, the coordinates of these points were marked on a WGS84 coordinate system. Furthermore, where occurrence records were lacking, precise geo-coordinates were obtained by using Google Earth (http://ditu.google.cn/) to determine latitude and longitude values (Xu et al. 2021). The distributional localities were compiled into a CSV database (.csv) using the sources mentioned above.

Bioclimatic (BC) and non-bioclimatic variables (NBC)

Climate change's impact on endangered plant species in terrestrial ecosystems is complex, and more information about potential distribution areas is needed to identify and rehabilitate them. Machine learning methods can be used to determine the current potential and future distribution of species based on records of point areas where species are currently present, as well as digital bioclimatic data for these areas (Sarikaya et al. 2018; Wei et al. 2018).

The sixth IPCC assessment report includes four climate change scenarios known as Shared Socioeconomic Pathways (SSPs): SSP1-2.6, SSP2-4.5, SSP3-7.0, and SSP5-8.5 (Meinshausen et al. 2020). We selected the SSP2-4.5 scenario, in which greenhouse gas emissions are roughly the same as they are now (1970–2000) and global average temperature tends to decrease with human intervention. The bioclimatic variables used to predict current and future distributions, with a spatial resolution of 30 s (~ 1 km^2) were derived from observational data in WorldClim ver. 1.4, which is available online at https://www.worldclim.org/data/index.html (accessed on 21st March 2022).

19 bioclimatic variables (Hijmans et al. 2005) for current as well as three future climatic scenarios (2050 time frame that represents the mean values from 2041 to 2060, 2070 represents the mean values from 2061 to 2080, and 2090 represents mean values from 2081 to 2100; Coban et al. 2020; Ye et al. 2020) were downloaded and clipped

from world data for India at a spatial resolution of 30 arc sec (~ 1 × 1 km resolution) and converted to ASCII (or ESRI ASCII) in DIVA-GIS version 7.5 (Zhang et al. 2021). Table 1 contains information on each bioclimatic parameter, including units and mathematical expressions.

Habitat heterogeneity index (HHI)

Because a more heterogeneous area may provide more niche space and allow more species to co-exist through niche partitioning, niche theory predicts a positive heterogeneity-diversity relationship. Tuanmu and Jetz (2015) developed 14 metrics to characterize global habitat heterogeneity at 1-km resolution based on the textural features of enhanced vegetation index (EVI) imagery from the Moderate Resolution Imaging Spectroradiometer (MODIS).

Six first-order and 8 second-order texture measures are accessible (http://www.earthenv.org/texture) at 30 arc-second (~ 1 km at the equator), 2.5 arc-minute (~ 5 km) and 12.5 arc-minute (~ 25 km) resolutions. In this study, we used 30 arc second data set related to first-order texture measures (coefficient of variation = normalized dispersion of EVI; evenness = evenness of EVI; range = range of EVI; Shannon and Simpson Indices = diversity of EVI; standard deviation = dispersion of EVI) and to second-order texture measures (uniformity = orderliness of EVI; maximum = dominance of EVI combinations.

Land use

Land use parameters like forest land, GRS (i.e. percent share of grass/scrub/woodland) and NVG (i.e. barren/very sparsely vegetated land) were downloaded from https://www.fao.org/soils-portal/soil-survey/soil-maps-and-databases/harmonized-world-soil-database-v12/en/ as recommended by Fischer et al. (2008).

Terrain slope and aspect

The global terrain slope and aspect database has been compiled using elevation data from the Shuttle Radar Topography Mission (SRTM). The SRTM data are publicly available as 3 arc second (approximately 90 m resolution at the equator) http://webarchive.iiasa.ac.at/Research/LUC/External-World-soil-database/HTML/global-terrain-slope.html?sb=6 (Fischer et al. (2008). In this study we utilized following parameters: (Aspect = East: 45° < aspect ≤ 135°; North: 0° < aspect ≤ 45° or 315° < aspect ≤ 360; West: 225° < aspect ≤ 315 and South: 135° < aspect ≤ 225°) and Slopes (Slope C1 = 0% ≤ slope ≤ 0.5%; Slope C2 = 0.5% ≤ slope ≤ 2%; Slope C3 = 2% ≤ slope ≤ 5%; Slope C4 = 5% ≤ slope ≤ 10%; Slope C5 = 10% ≤ slope ≤ 15%; Slope C6 = 15% ≤ slope ≤ 30%; Slope C7 = 30% ≤ slope ≤ 45%; Slope C8 = Slope ≥ 45%).

Table 1 Description of predictive bioclimatic variables used in this study (downloaded from WorldClim related to four time frames: current, 2050, 2070 and 2090 of Shared Socioeconomic Pathways (SSP2-4.5 scenario)

Code	Environmental variables and their abbreviations	Scaling factor	Unit
BC-1	Annual mean temperature (AMT)	10	°C
BC-2	Mean diurnal range (MeDR)	10	°C
BC-3	Isothermality (BC-2/BC-7) (×100) (Iso)	100	–
BC-4	Temperature seasonality (standard deviation × 100) (TempS)	100	–
BC-5	Max temperature of warmest month (MaTWaM)	10	°C
BC-6	Min temperature of coldest month (MiTCM)	10	°C
BC-7	Temperature annual range (BC-5 – BC-6) (TAR)	10	°C
BC-8	Mean temperature of wettest quarter (MeTWeQ)	10	°C
BC-9	Mean temperature of driest quarter (MeTDQ)	10	°C
BC-10	Mean temperature of warmest quarter (MeTWaQ)	10	°C
BC-11	Mean temperature of coldest quarter (MeTCQ)	10	°C
BC-12	Annual precipitation (AnPr)	1	mm
BC-13	Precipitation of wettest month (PrWeM)	1	mm
BC-14	Precipitation of driest month (PrDM)	100	mm
BC-15	Precipitation seasonality (coefficient of variation) (PrS)	1	Fraction
BC-16	Precipitation of wettest quarter (PrWeQ)	1	mm
BC-17	Precipitation of driest quarter (PrDQ)	1	mm
BC-18	Precipitation of warmest quarter (PrWaQ)	1	mm
BC-19	Precipitation of coldest quarter (PrCQ)	1	mm

Soil qualities

Nutrient availability, rooting conditions, nutrient retention capacity, oxygen availability to roots, excess salts, and toxicity were downloaded and used. Nutrient availability (as it relates to soil texture, organic carbon, pH, and total exchangeable bases), rooting conditions (soil textures, bulk density, coarse fragments, vertic soil properties and soil phases affecting root penetration and soil depth and soil volume). Furthermore, rooting conditions include effective soil depth (cm) and effective soil volume (vol. percent) in relation to the presence of gravel and stoniness. Nutrient retention capacity (soil organic carbon, soil texture, bases saturation, cation exchange capacity, and clay fraction), oxygen availability to roots (soil drainage and soil phases influencing soil drainage), excess salts (explains soil salinity, soil sodicity, and soil phases influencing salt conditions), and toxicity (calcium carbonate and gypsum) were downloaded (Fischer et al. 2008; https://www.fao.org/soils-portal/data-hub/soil-mapsdatabases/harmonized-world-soil-database-v12/en/).

In this study, we followed the advice of Zhao et al. (2021), who stated that land use, soil, and HHI-related parameters are unlikely to change significantly in the near future; therefore, we used these NBC in conjunction with different bioclimatic time-frame datasets to examine the cumulative impacts of both such predictors on the habitat suitability of this species.

Data processing

Issue of multicollinearity

The multicollinearity test was used in this study to reduce the risk of over-fitting by examining the cross-correlation with Pearson Correlation Coefficient (*r*). Furthermore, variables with cross-correlation coefficient values greater than 0.85 were excluded stepwise (Pradhan 2016). Niche Tool Box (Osorio-Olvera et al. 2020 https://github.com/luismurao/ntbox) was used for this analysis.

One of two highly cross-correlated variables was chosen because it is biologically related to the species and provides comfort in model interpretation (Kumar et al. 2006; Kumar and Stohlgren 2009; Padalia et al. 2014). In this manner, only one variable from each set of highly cross-correlated variables ($r^2 > 0.85$) was kept (Ma and Sun 2018). In this study, 70% and 30% of the data were assigned to model training and validation, respectively (Mousazade et al. 2019).

Projection assignment and their transformations

Because the bioclimatic (BC) and non-BC variables were obtained from different sources and at different resolutions, their projections should be corrected before extracting data and predicting the ensemble model. This was accomplished in this study through the use of a series of steps in ArcMap using ArcToolbox. First, we defined the projection in Data Management Tools' "projection and transformation" sub-window. We used the WGS 1984 EASE Geographic Coordinate System (GCS) for this. However, to quantify area under each habitat suitability class (as explained below), the "calculate geometry" window of ArcMap requires a Projected Coordinate System (PCS), hence, we converted the projections of habitat class raster file to WGS 1984 web Mercator (auxiliary sphere-3857). This step allows us to calculate area under specific class with a user-specified unit (we utilized square kilometre).

Species distribution modelling

Maxent 3.4.1 software (available at http://www.cs.princeton.edu/schapire/Maxent/) was used in this study to simulate and predict the potential geographical distribution probability of *C. wightii* under the current (Rong et al. 2019; Mishra et al. 2021) and three future scenarios (Coban et al. 2020; Ye et al. 2020). In this paper, we presented our Maxent output at three different levels: (a) non-colinear BC variables (with Current, 2050, 2070, and 2090 time frames), (b) non-colinear non-bioclimatic variables, and (c) combination of significant variables related to BC and NBC.

During the modelling process, 70% of the distribution data samples of *C. wightii* were randomly selected as training data, and 30% of the samples were used as testing data. The number of randomly generated background points was set to 10,000 (Zhang et al. 2021). We set the regularization multiplier to 0.1 to avoid over-fitting of the test data (Phillips and Dudik 2008). Linear, quadratic, and hinge properties were employed. For model building, a total of 100 runs were planned (Flory et al. 2012). We used the Jackknife method in the environment parameter settings, and the other parameter settings were set to the software default values. Threshold-independent receiver operating characteristic (ROC) analyses were used to calibrate and validate the robustness of Maxent model evaluation, and an area under the receiver operating curve (AUC) was used to estimate the accuracy of the model predictions (Elith et al. 2006). The model's performance was graded as failing (0.5–0.6), poor (0.6–0.7), fair (0.7–0.8), good (0.8–0.9), or excellent (0.9–1). AUC values near one indicate that the model is performing well.

Species' niche hypervolumes

ENM analysis was performed to better understand the behaviour of this species' hypervolumes in relation to various factors. Maxent modelling provides significant variable importance for distribution of this species with different BC and NBC parameters. For ecological niche

analysis, we used the first three most important variables/contributors from each Maxent analysis. Only NBC variables with AUCs greater than 0.80 were taken into account. NicheToolBox was used for the ENM (Ntbox Osorio-Olvera et al. 2020). Ntbox is a Graphical User Interface (GUI) tool based on the R programming language that requires raster output of BC or NBC variables. Ellipsoidal models were built using the centroid and covariance matrix of this species' environmental values. From the centroid to each environmental combination in the study area, Mahalanobis distances (MD) were calculated. Suitability values (S) were calculated by constructing a multivariate normal distribution from MD; $S \sim \exp(-0.5 \times MD)$ and assuming that the highest suitability values were closer to the centroid (Nunez-Penichet et al. 2021). The application of various regression curves was used to assess the relationships between MDs and the suitability and projected geographical abundance of this species.

Habitat suitability classes

The habitat of *C. wightii* was divided into four categories based on values (0 to 1): optimal (0.80 to 1), moderate (0.60 to 0.80), marginal (0.40 to 0.60), and low (0.20 to 0.40). Area ($\times 10^4$ km^2) under these classes, as well as area gain and loss between two time frames (for BC variables) were calculated in ArcMap using the raster calculator tab (spatial Analyst Tool/Map Algebra/Raster Calculator). We also calculated percent changes in mean habitat suitability using the formula (Mathur and Sundarmoorthy 2013; Mathur 2014a, b; Kaky and Gilber 2019):

$$\left[\left(\frac{(\text{Future}-\text{Current})}{\text{Current}}\right) \times 100\right].$$

Changes in core distribution centres

The SDM toolbox was used to assess centroid shifting between different bioclimatic time frames (Brown and Anderson 2014). This tool computes the distributional changes between two binary SDMs (current vs. future SDMs), producing a table output depicting the predicted contraction, expansion, and areas of no change in the distribution of a given species (Brown et al. 2017).

Niche overlap

In the present day, niche overlap compared the inferred and true distributions of suitability scores across geographic space. The Maxent output in ASCII format of each analysis was used to quantify niche overlap between two studied parameters (related to BC, NBC, and BC + NBC). ENMTools was used to accomplish this (Warren et al. 2010). The purpose of this analysis was to visualize the amount of area retained by this species under various predictions. To represent the ecological niche overlap, Schoener's *D* (which measures the consistency of niche overlap per pair) and Hellinger's-based *I* (which measures the degree of overlap of the geographical distribution) values were used. *D* and *I* values ranged from 0 to 1. With the increase in the value, the ecological niche overlap would be improved (Ahmad et al. 2019). The following classes were used to facilitate interpretation of niche overlap based on *D* values: 0–0.2 = no or very limited overlap, 0.2–0.4 = low overlap, 0.4–0.6 = moderate overlap, 0.6–0.8 = high overlap, 0.8–1.0 = very high overlap (Wan et al. 2017).

Automated conservation assessments

Using our spatially thinned geographical locations, we first investigated the current status of *C. wightii*. We calculated the extent of occurrence (EOO, km^2), the area of occupancy (AOO, km^2), the number of unique occurrences, the number of subpopulations, the number of locations, the IUCN (2014) threat category according to Criterion B, and the IUCN annotation (Category Code) using the R programme "ConR" (Dauby et al. 2017; Kass et al. 2021). In addition, we performed a similar exercise to assess the impact of niche modelling on EOO and AOO using the Maxent output for each variable and their combinations. Using ArcMap, we convert the ASCII format into a "XYZ" file. This file was then converted to a text file and opened in Microsoft Excel. Because these maps are the projected output of an ENM analysis, hence to reduce issue of over-fitting we chose only coordinates with up to moderate habitat suitable categories for estimation of EOO and AOO using ConR software. Such approaches were advocated by Marcer et al. (2013), Adhikari et al. (2018) and Marco et al. (2018). Number of sub-populations and locations were estimated by standard methodology as provided by Mathur and Mathur (2023).

Results

Data processing and multicollinearity

We were able to extract 268 geographical locations of this species from various sources, which were primarily concentrated in the Indian states of Rajasthan and Gujarat. Using the Spatial Thin window of the R-based Graphical User Interface Wallace Software, duplicate records were filtered spatially and deleted to keep only one occurrence (Kass et al. 2018). Finally, 144 *C. wightii* presence records were obtained in order to construct the ENM.

We use the procedures described by Kumar et al. (2006) and Pradhan (2016) to address the issue of multicollinearity in species distribution modelling. Significant correlation values (r^2) between different variables are presented in Additional file 1: Fig. S1a (Current), 1b (2050

BC), 1c (2070 BC) and 1d (2090 BC). Similarly, correlation analysis for non-bioclimatic parameters, soil, slope and aspect, land use and habitat heterogeneity indices are presented in Additional file 1: Tables S1–S4, respectively. Table 2 shows the variable importance values for bioclimatic variables related to different climatic time frames used for ENM analysis. Furthermore, variables excluded due to their significant correlations with other variables are denoted in Table 2 with the symbol "×".

Model performances

The area under the receiver operating curve (AUC) was used to assess the performance of the Maxent model for species distribution prediction. We observed that this machine learning tool performs excellently (both for training and test data, AUC = 0.9–1.0) with all bioclimatic time frames (Fig. 2) and for soil, slope, and aspect (training data AUC > 0.91) while model qualities were good with HHI and land use variables. However, the combination of BC + NBC reduced our model's qualities to fair, as their respective AUC values were < 0.81 (Fig. 3).

Table 2 depicts the percent contribution (or variable importance percentage) of various bioclimatic variables over different time periods. With the current bioclimatic scenario, precipitation of the coldest quarter (BC-19, VIP = 49.7), precipitation seasonality (BC-15, VIP = 18.1), and maximum temperature of the warmest month (BC-5, VIP = 13.8) were identified as most crucial factors for this species, while temperature annual range (BC-7, VIP = 0.3) and precipitation of driest month (BC-14, VIP = 1.7) were the least effective factors for its habitat suitability during this time period. Precipitation seasonality (BC-15, VIP = 55.1) was identified as the most important factor for habitat suitability of this species with 2050 time frame followed by precipitation in the driest quarter (BC-17, VIP = 13.6). Our analysis revealed that mean diurnal range (BC-2, VIP = 2.5) and isothermality (BC-3, VIP 2.5) will be the least effective factors for this species during this time period (Table 2). With 2070 climatic time frame, we noticed the effective role of precipitation of the coldest quarter (BC-19, VIP = 46.9), precipitation of the wettest month (BC-13, VIP 14.7) and precipitation seasonality (BC-15, VIP 14.1), while mean diurnal range, temperature seasonality and annual precipitation were identified as least effective variables.

With 2090 time frame, we noticed roughly equal contribution of mean temperature of wettest quarter (BC-8, VIP 17.6), Isothermality (BC-3, VIP 14.4), and precipitation of wettest quarter (BC-16, VIP = 13.4), while the mean temperature of the driest quarter (BC-9, VIP 1.7) and precipitation of the driest month (BC-14, VIP 1.7) were recognized as least effective factors (Table 2).

Table 3 shows the percent contribution of various non-bioclimatic variables. Excess salt (which explains soil salinity, soil sodicity, and soil phases influencing salt conditions) was the most effective variable (VIP = 75.3) that influenced the distribution of this species, followed by rotting condition (VIP = 20.3) that revealed the effective soil depth (cm) and effective soil volume (vol. percent) related to the presence of gravel and stoniness. The least effective factors were nutrient and oxygen availability.

Our findings indicated that slope 6 (15% ≤ slope ≤ 30%), slope 1 (0% ≤ slope ≤ 0.5%), slope 7 (30% ≤ slope ≤ 45%) and slope 2 (0.5% ≤ slope ≤ 2%) had the greatest influence among terrain slope and aspect variables, in decreasing order. When compared to south and west, the east and north aspects were the most influential (Table 3). GRS (VIP = 86.5), which denotes the percent share of grass/scrub/woodland, was identified as the most effective factor for this species among land use variables (Table 3). Similarly, range (VIP = 39.5) was identified as the most important variable among habitat heterogeneity variables, followed by coefficient of variation (VIP = 19.2) and maximum (VIP = 18.4), while standard deviation (VIP = 3) and evenness (VIP = 2.5) were the least influential.

Table 2 Percentage contribution (or variable importance percentage) calculated using four climate time frames

Climatic variables	VIP of different variables with four climatic time frames			
	Current	2050	2070	2090
AMT	2.9	5.6	1.5	×
MeDR	3.8	2.5	1.1	×
Iso	3.6	2.5	2.2	14.4
TempS	2.6	4.8	1.5	×
MaTWaM	13.8	5.6	2.6	×
MiTCM	3.5	×	×	7.9
TAR	0.3	×	×	3.4
MeTWeQ	×	×	×	17.6
MeTDQ	×	×	×	1.7
MeTWaQ	×	×	×	12.9
MeTCQ	×	×	×	×
AnPr	×	×	1.6	×
PrWeM	×	×	14.2	4.3
PrDM	1.7	×	×	1.7
PrS	18.1	55.1	14.7	3.8
PrWeQ	×	3.2	×	13.4
PrDQ	×	13.6	2.4	3.3
PrWaQ	×	7.3	11.3	5.3
PrCQ	49.7	×	46.9	10.4

Bioclimatic variables with higher VIP values were then used as predictors alongside highly contributed non-bioclimatic variables to establish a link between species distribution and their environment

×: variables excluded due to their significant correlations with other variables

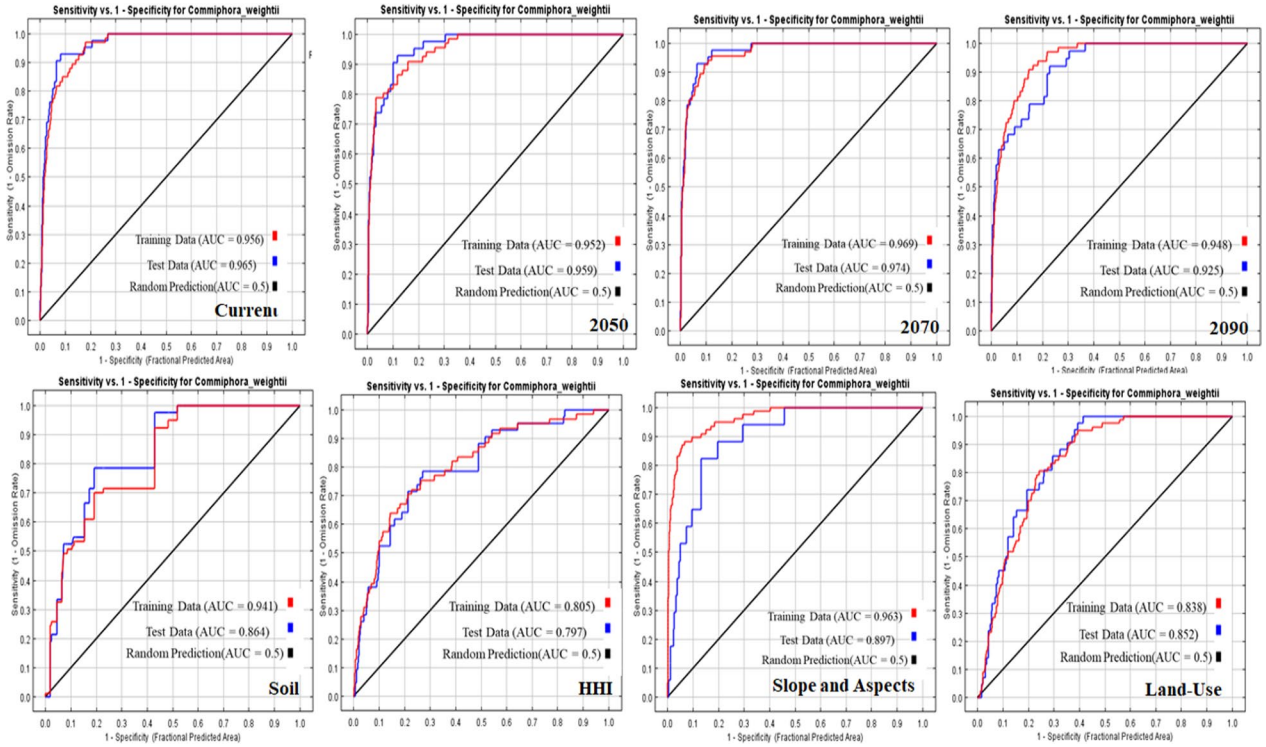

Fig. 2 Area under receiver operating characteristics curve (AUC) graphs for model performance (both training and test data set) belongs to four bioclimatic (current, 2050; 2070 and 2090) and four non-bioclimatic variables (soil, habitat heterogeneity indices, slope and aspects and land use)

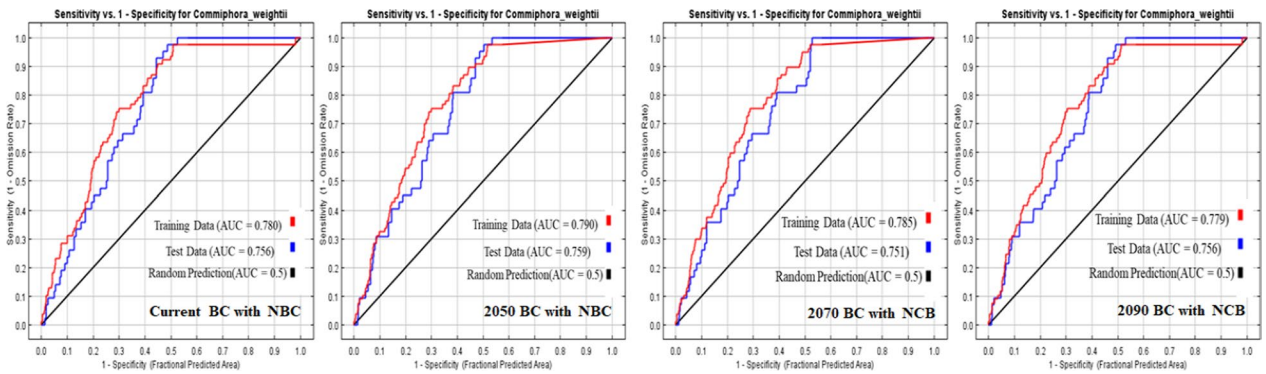

Fig. 3 Area under receiver operating characteristics curve (AUC) graphs for model performance (both training and test data set) belongs to combination of bioclimatic and non-bioclimatic variables (soil, habitat heterogeneity indices, slope and aspects and land use)

The coefficient of variation is the most influential factor for this species across all combination types, according to the percent contribution of different variables calculated with Maxent BC + NBC (Table 4). Its significance was greater than 95% when the NBC was combined with the current, 2070, and 2090 bioclimatic time frames. However, with 2050 + NBC, its percent contribution (VIP = 49) to this species' distribution was shared with precipitation seasonality (VIP = 36.8) and rooting conditions (VIP = 6.3).

Response curves illustrating the effects of predictors on occurrence probability

Species response curves depict the relationships between environmental factors and the likelihood of occurrence of a species. They demonstrate target species' biological tolerances and habitat preferences. Response curve during current climatic time frames reveal existence of lowest *C. wightii* population with low value of precipitation of the coldest quarter (Fig. 4a). This bioclimatic variable basically provides the total precipitation (mm) during

Table 3 Percentage contribution (or variable importance percentage) of various non-bioclimatic variables

Variables	PC	Variables	PC
Soil qualities		Land use	
Excess salt	75.3	GRS	86.5
Rooting conditions	20.3	Forest cover	7.2
Nutrient availability	3.4	NVG	5.6
Oxygen availability to root	1	Habitat heterogeneity variables	
Terrain slope and aspect variables		Range	39.5
Slope 6	23.7	Coefficient of variation	19.2
Slope 1	19.2	Maximum	18.4
Slope 7	18.7	Uniformity	11.4
Slope 2	17.9	Shannon diversity	6.1
East aspect	5.1	Standard deviation	3
Slope 4	4.8	Evenness	2.5
Slope 5	3.7		
North aspect	2.3		
South, West aspect, Slope 3	1.1		

Variables with higher VIP values were then used as predictors alongside highly contributed bioclimatic variables to establish a link between species distribution and their environment

PC: percent contribution; GRS (percent share of grass/scrub/woodland); NVG (barren/very sparsely vegetated land)

Table 4 The percentage contribution (or variable importance percentage) of various bioclimatic and non-bioclimatic (NBC) variables was calculated by combining the highest VIPs of BC and NBC for the respective time frame

Variables	PC	Variables	PC
Current and NBC		2070 and NBC	
Coefficient of variation	95.9	Coefficient of variation	98.4
Excess salt	3.0	PrS	0.6
2050 and NBC		2090 and NBC	
Coefficient of variation	49.0	Coefficient of variation	95.9
PrS	36.8	Excess salt	3.0
Rooting conditions	6.3		

Variables with higher VIP values were used to connect species to their environment

PC: percent contribution; PrS: precipitation seasonality

the coldest three months of the year. Under prevailing climatic scenario, 1–11 mm PrCQ is the threshold value for the habitat suitability of this species and we noticed subsequent decrease in the predicted value of this species with the higher PrCQ.

Precipitation seasonality (BC-15, coefficient of variation) reflects rainfall variability, with higher percentages indicating greater precipitation variability (Fig. 4b). According to our findings, the optimum habitats of this species are supported with precipitation with a range of 140–170 mm and then sharply decreased (Fig. 4b). We observed a sharp increase in species response at 38° to 42 °C during the warmest month (BC-5), and then its presence declined sharply (Fig. 4c). Precipitation seasonality (BC-15) was also identified as the most important factor during BC-2050, and our findings indicated nearly similar trends for this species' suitability with this bioclimatic variable (Fig. 5a). Figure 5b and c shows ROC curves for the BC-2050 time frames with precipitation of driest quarter (BC-17) and precipitation of warmest quarter (BC-18). Analysis revealed that a small amount of precipitation (up to 10 mm) during the driest quarter facilitates the suitability of this species, while the warmest month precipitation (BC-18, up to 200 mm) supports this species.

During 2070 BC, we observed that precipitation of the coldest quarter (BC-19), precipitation of the wettest month (BC-13), and precipitation seasonality (BC-15) were the most important influencing factors for this species' suitability. BC-19 exhibited similar trends to those observed during the current climatic time frame (Fig. 6a). Precipitation in the wettest month supports this species and is optimized at 200 mm, remains constant up to 400 mm, and then sharply declines (Fig. 6b). Furthermore, the best suitability with precipitation seasonality was found to be between 140 and 160 mm (Fig. 6c).

We found that this species was most suitable in 2090 BC, when the mean temperature of the wettest quarter (BC-8) ranged between 10 and 15 °C, and then declined (Fig. 7a). The percentage ratio of mean diurnal range/annual temperature range is referred to as isothermality (i.e. the ratio of mean diurnal temperature range to annual temperature range 100). A site with an isothermality value of 100 has the same diurnal temperature range as the annual temperature range. Values less than 100 indicate a lower level of diurnal temperature variability (mean of monthly (maximum–minimum temperature)) compared to yearly temperature variability (maximum temperature of warmest month–minimum temperature of coldest month).

In this study, we found that isothermality (2090 BC) from 0.25 to 0.30 is ideal for this species, and its population began to decline but in a rhythmic and consistent manner at 22 to 32 (Fig. 7b). Figure 7c depicts the ROC curve for the wettest quarter during the 2090 BC time frame. The results showed a gradual increase in suitability with this climatic parameter up to 290 mm, with a peak of suitability at 300 mm (Fig. 7c).

Among the soil quality parameters, excess salt has the greatest influence on the occurrence probability of this species. The optimum range of this environmental factor was 0.5 to 3.5 dS/m, and the occurrence significantly decreased after that (Fig. 8a). We found that rooting

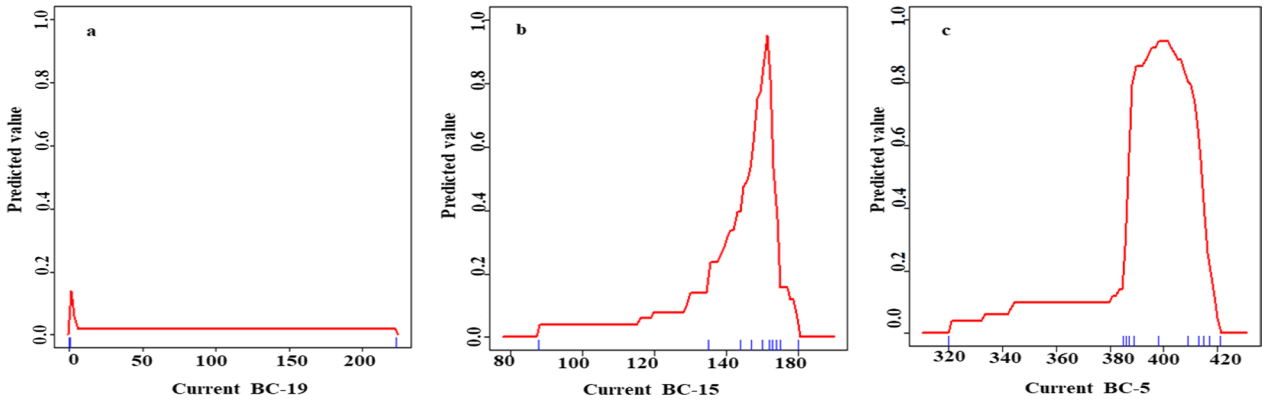

Fig. 4 Receiver operating characteristics curve (ROC) illustrating relationship between probability of occurrence of suitable conditions for distribution of *C. wightii* with most significant bioclimatic predictor during current time frame: **a** PrCQ, **b** PrS and **c** MaTWaM

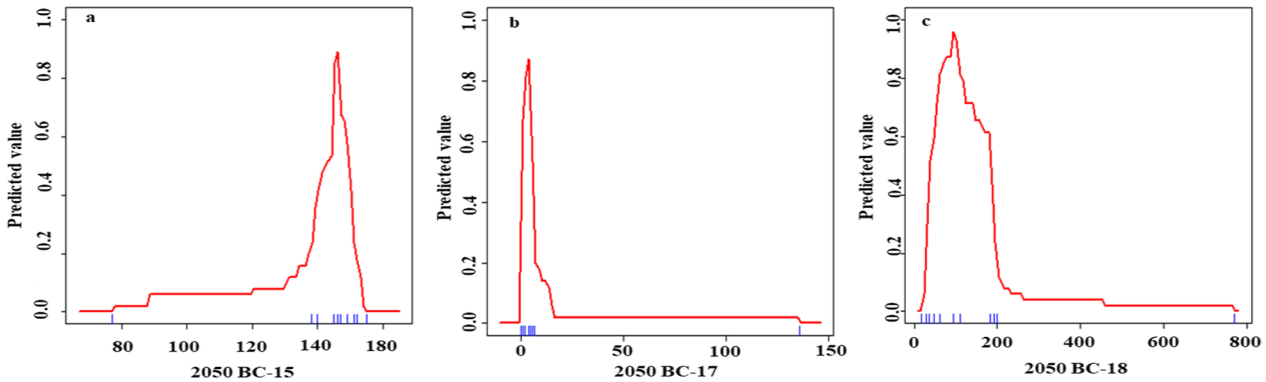

Fig. 5 Receiver operating characteristics curve (ROC) illustrating relationship between probability of occurrence of suitable conditions for distribution of *C. wightii* with most significant bioclimatic predictor during 2050 time frame: **a** PrS, **b** PrDQ and **c** PrWaQ

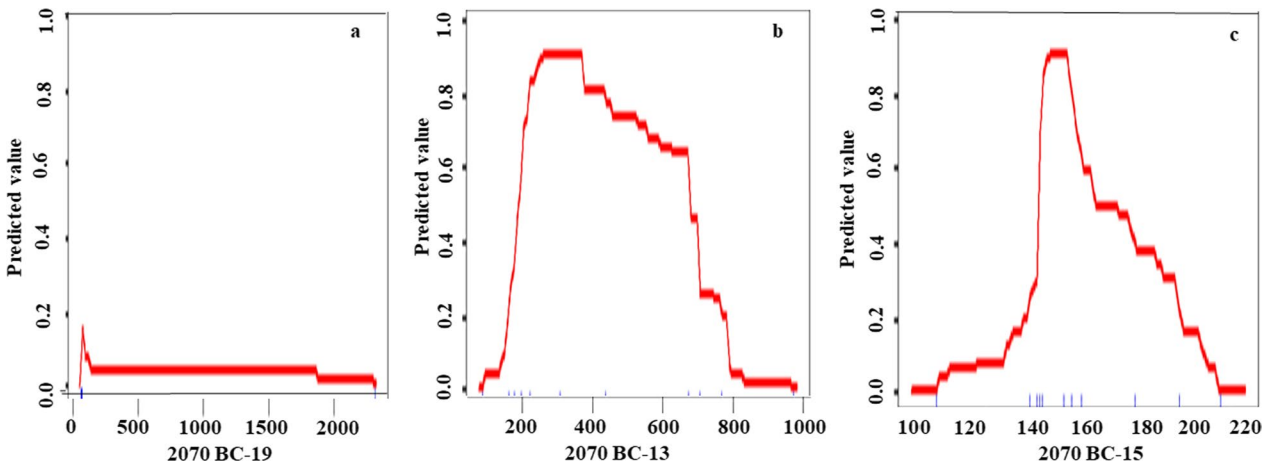

Fig. 6 Receiver operating characteristics curve (ROC) illustrating relationship between probability of occurrence of suitable conditions for distribution of *C. wightii* with most significant bioclimatic predictor during 2070 time frame: **a** PrCQ, **b** PrWeM and **c** PrS

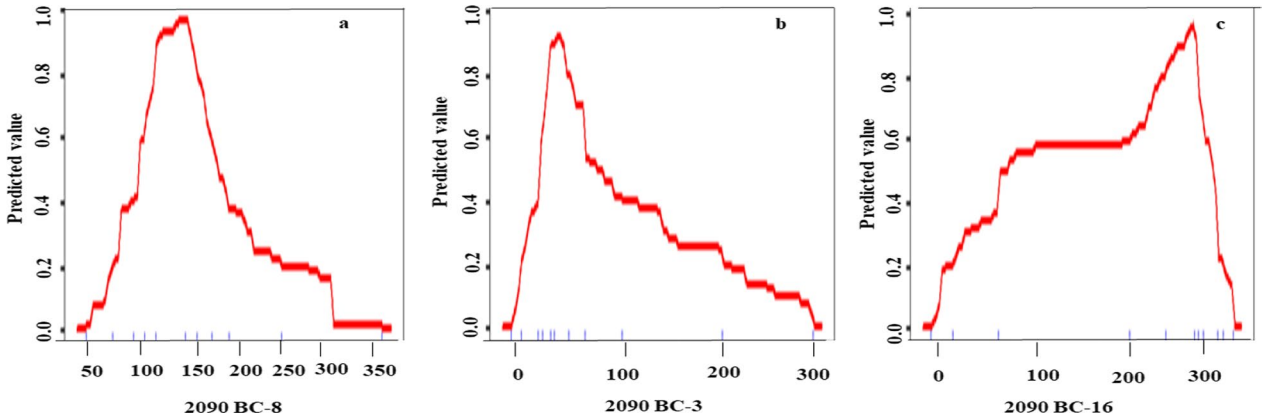

Fig. 7 Receiver operating characteristics curve (ROC) illustrating relationship between probability of occurrence of suitable conditions for distribution of *C. wightii* with most significant bioclimatic predictor during 2090 time frame: **a** MeTWeQ, **b** Iso and **c** PrWeQ

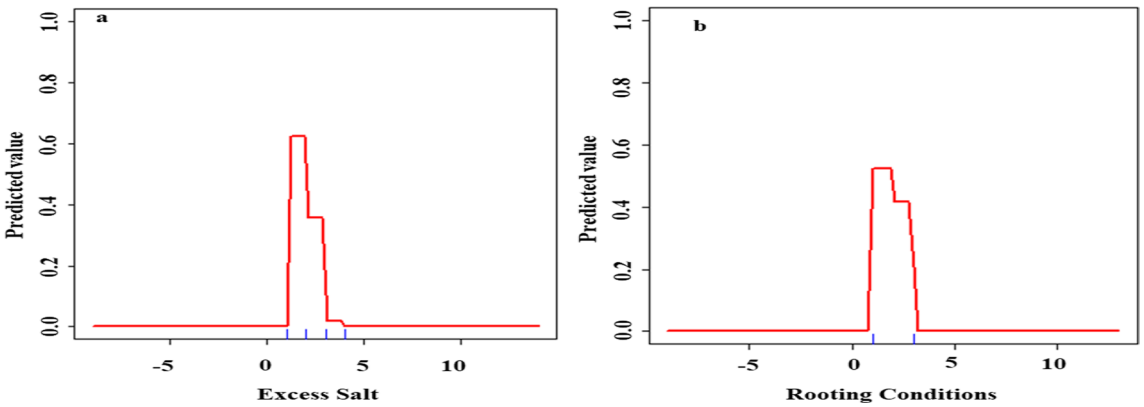

Fig. 8 Receiver operating characteristics curve (ROC) illustrating relationship between probability of occurrence of suitable conditions for distribution of *C. wightii* with most significant soil quality predictors excess salt (**a**) and rooting conditons (**b**)

conditions ranging from 0.5 to 3.5 were the most suitable for this species, and that above this limit, the occurrence probability decreased (Fig. 8b). The maximum probability of occurrence with range textural measure was recorded between 350 and 420 (Fig. 9a), while this peak was attended at 150–180 with coefficient of variation (Fig. 9b) and 100–400 with maximum variable (Fig. 9c). With these textural habitat heterogeneity variables, the maximum probability of occurrences of this species was sharply reduced after exceeding peak values.

Among the land use parameters, the percent share of grassland/scrub/woodland (GRS) was the most significant variable affecting its occurrence probability, and our response curve suggested a maximum probability beyond 1% and stabilized up to 100% share of GRS (Fig. 10).

This species' occurrence probability is affected by slopes 6, 1, and 7 (Figs. 11a, b, c, respectively). All of these variables demonstrated that this species can occur from 0.5 percent slope (slope 1) to 45 percent slope (slope 7).

Species' niche hypervolumes

The ecological niche can be viewed as a volume in multidimensional space, with each dimension describing an abiotic condition or biotic resource that a species requires. Niche hypervolume was also analysis to better understand the behaviour of this species' hypervolumes in relation to various factors. Table 5 shows the Mahalanobis distances (MD), suitability, and projected geographical abundance of this species. Furthermore, we did not conduct this analysis for land use because a single individual variable, GRS, demonstrated dominance over other variables (forest cover and NVG) with VIP = 86.5. Similarly, we did not include the soil variable because there is a significant difference in VIP between the first three variables (Table 3). We can categorize the probability of occurrence as optimal (> 0.80), moderate (0.60–0.80), marginal (0.35–0.60), and low (0.15–0.30) based on suitability values. Highest suitability values were closer to the centroid (Nunez-Penichet

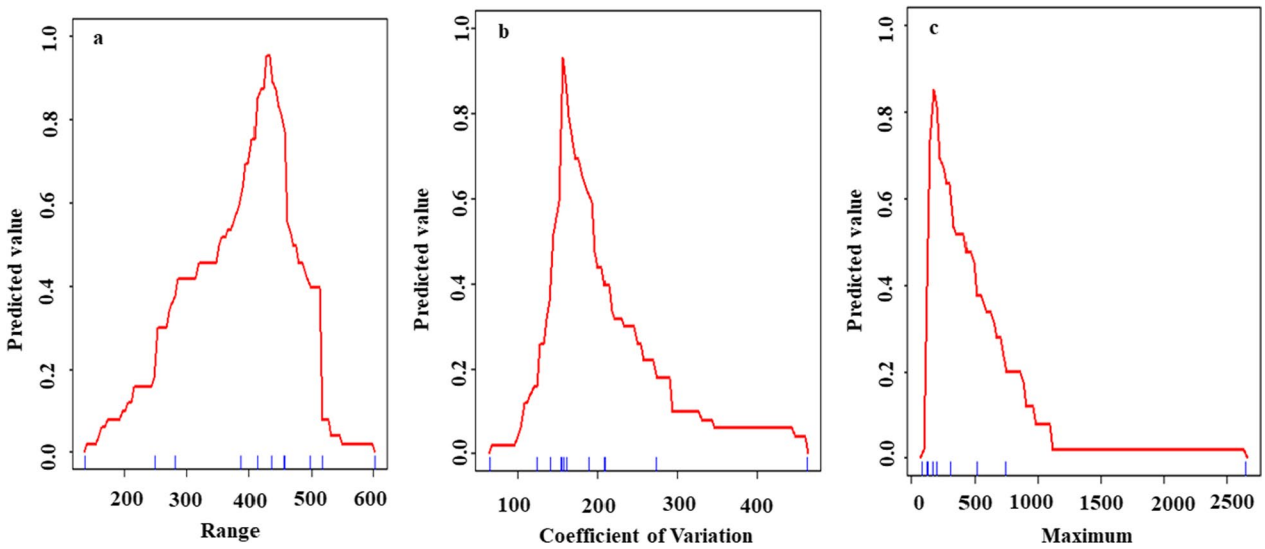

Fig. 9 Receiver operating characteristics curve (ROC) illustrating relationship between probability of occurrence of suitable conditions for distribution of *C. wightii* with most significant habitat heterogeneity predictors like range (**a**) coefficient of variation (**b**) and maxium (**c**)

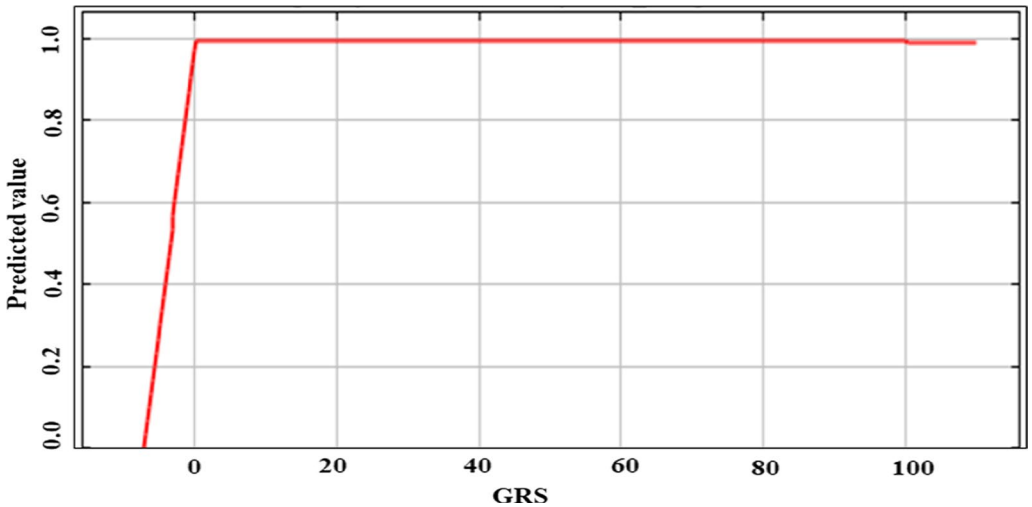

Fig. 10 Receiver operating characteristics curve (ROC) illustrating relationship between probability of occurrence of suitable conditions for distribution of *C. wightii* with most significant land use predictor GRS (percent share of grassland/scrub/woodland)

et al. 2021), and we found a significant negative linear relationship between MD and suitability with individual BC and NBC (Table 5) as well as with combined inclusion of both variables pertains to BC and NBC ($R^2 = 0.97$; Additional file 1: Fig. S2). Projected geographical abundance also revealed significant negative power relationship with suitability (Additional file 1: Fig. S3) that can be equate as Suitability $= 2.07 \times$ Geographical Abundance$^{\wedge -0.22}$; $R^2 = 0.637$ ($P = 0.01$). There were no such relationships found between Mahalanobis distances and geographical abundance.

In terms of bioclimatic space, *C. wightii's* ellipsoidal niche had a larger hypervolume (55.41×10^4 °C·mm^2) during BC-2090, followed by BC-2070 (11.34×10^3 °C·mm^2), and was the smallest during the current scenario (29.81×10^1 °C·mm^2). Among all BC and NBC variables, slopes (75.70×10^6 °C·mm^2) and HHI (71.83×10^6 °C·mm^2) produced the highest hypervolume.

The influence of environmental variables on niche dynamics is indicated by their centroid values. Their proximity to the centroid indicates that they exert control over species suitability (Nunez-Penichet et al. 2021). Figures 12 and 13 show a graphical representation of

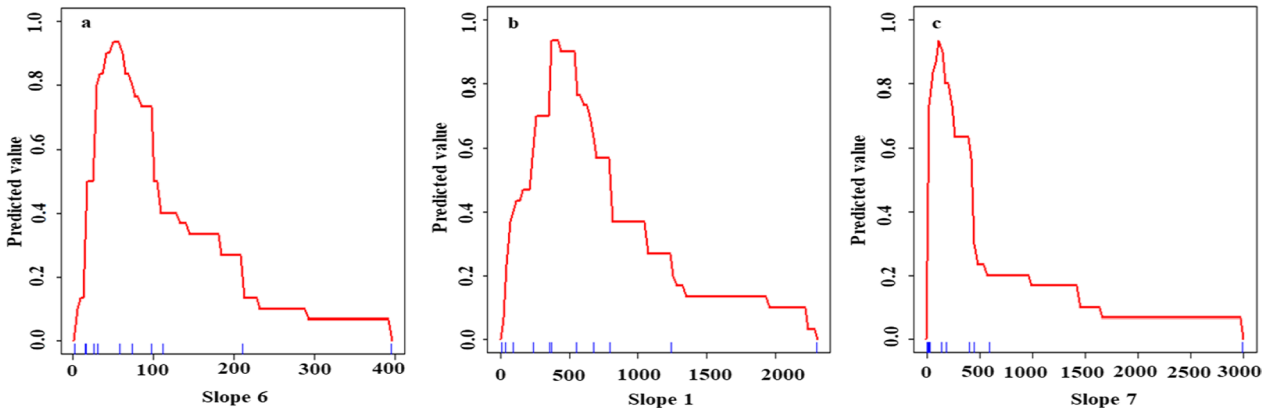

Fig. 11 Receiver operating characteristics curve (ROC) illustrating relationship between probability of occurrence of suitable conditions for distribution of *C. wightii* with most significant slope types slope 6 (**a**), slope 1 (**b**) and slope 7 (**b**)

Table 5 Values of ecological niche modelling attributes classified under four habitat suitability classes of *C. wightii*

Variables	Optimum	Moderate	Marginal	Low
C-MD	0.25	0.90	1.85	3.36
C-Sui	0.88	0.64	0.40	0.20
C-GA	98.0	273.0	312.0	482.0
50-MD	0.24	0.90	1.84	3.28
50-Sui	0.88	0.64	0.40	0.20
50- GA	62.0	311.0	510.0	699.0
70-MD	0.23	1.00	1.80	3.37
70-Sui	0.89	0.60	0.40	0.19
70-GA	30.0	213.0	438.0	624.0
90-MD	0.25	0.93	1.83	3.40
90-Sui	0.87	0.63	0.40	0.19
90-GA	261.0	994.0	1312.0	2715.0
HHI-MD	0.30	1.15	1.47	3.30
HHI-Sui	0.86	0.66	0.43	0.20
HHI-GA	99.0	1512.0	1856.0	1679.0
Slope-MD	0.26	0.93	1.80	3.25
Slope-Sui	0.87	0.63	0.41	0.21
Slope-GA	745.0	5196.0	5249.0	5268.0

C: Current; 50 = 2050; 70 = 2070; 90 = 2090; MD: Mahalanobis distances; Sui: suitability and GA: geographical abundance

niche hypervolume with studied variables. The blue colour represents niche stability, the green colour represents niche unfilling (the proportion of the native niche that does not overlap with the exotic niche), and the red colour represents niche expansion (Ahmed et al. 2019). The size of these zones corresponds to the volume of their niche. With current BC, this species demonstrated the greatest niche expansion from its fundamental niche with maximum temperature of the warmest month (BC-5, i.e. energy variable), while precipitation seasonality (BC-15, water availability), and precipitation of the coldest quarter (BC-19) was identified as a facilitator to maintain its fundamental niche areas (Fig. 12). Precipitation seasonality will be the most important factor for its expansion in areas in the future (2050), followed by other water availability parameters such as precipitation of the warmest quarter (BC-18), while the fundamental niche will be operated by precipitation of the driest quarter (BC-17). As a result, we can predict that in the future (2050), both the establishment of this species in its natural habitat and its expansion/dispersal in new areas will be governed by water availability (Table 6). Similar water availability operating behaviour was observed with BC-2070, where BC-19 (PrCQ) will be the controlling factor for its fundamental niche and its expansion will be favoured with BC-13 (PrWeM) and BC-15 (Fig. 12). Our third future bioclimatic projection (BC-2090, Table 6) revealed the significance of the energy variable Isothermality (BC-3) for its fundamental niche, while its expansion will be governed by both energy (mean temperature of the wettest quarter, BC-8) and water availability (precipitation of wettest quarter, BC-16). With NBC, the range of EVI and the coefficient of variance of EVI (CV) were identified as the most important factors for its expansion into newer areas (Fig. 13), while the centroid will be maintained by the maximum of EVI (Table 6). The slopes with the greatest expansion were slopes 1 and 6 (Fig. 13).

Habitat suitability classes

We used the ArcMap tool to interpret Maxent's ASCII output (Raster projection and raster calculation) and categorized the probability of occurrence of this species into four suitability classifications. Tables 7 and 8 show the area ($\times 10^4$ km^2) of each suitability class with different bioclimatic and non-bioclimatic variables, as well as the combination of BC + NBC. Figure 14 a to d depicts

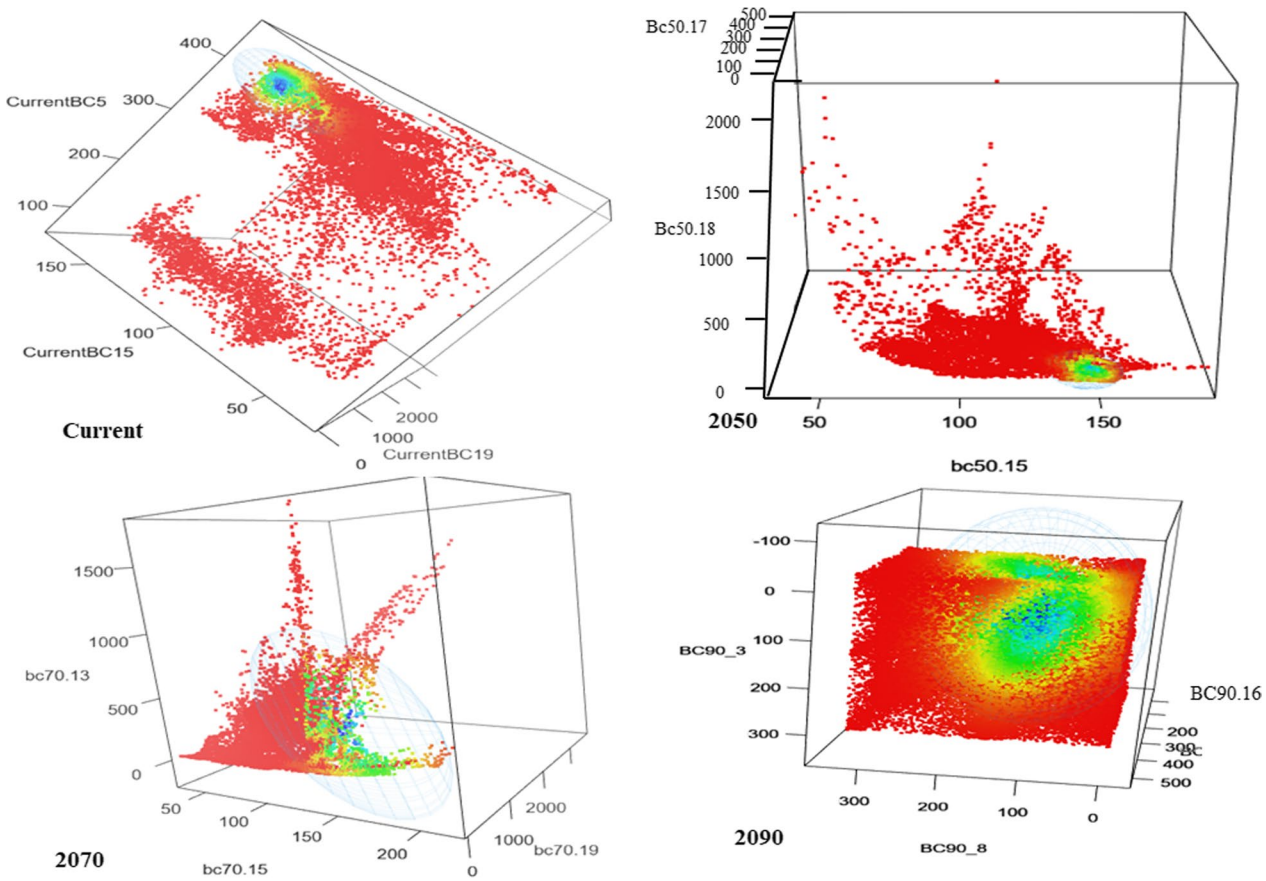

Fig. 12 Graphical representation of *C. wightii* niche hypervolume with three most influential bioclimatic variables pertains to four climatic projections (current, 2050, 2070 and 2090). The blue colour represents niche stability, the green colour represents niche unfilling (the proportion of the native niche that does not overlap with the exotic niche), and the red colour represents niche expansion

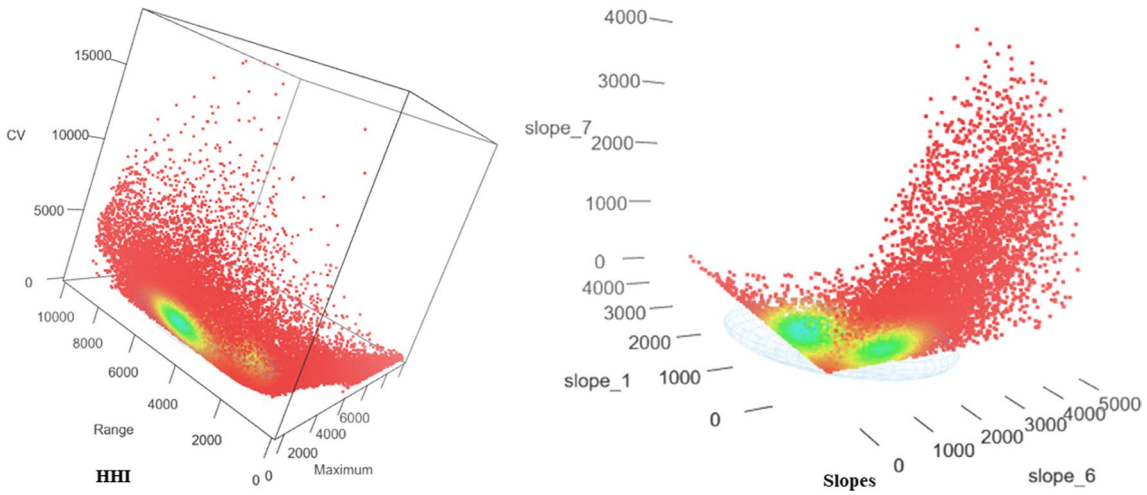

Fig. 13 Graphical representation of *C. wightii* niche hypervolume with three most influential variables pertains to non-bioclimatic predictors (habitat heterogeneity and slopes)

Table 6 Values of centroid of different environmental attributes pertains to various bioclimatic and non-bioclimatic predictors

Environmental variables	Current	2050	2070	2090	HHI	Slopes
BC-19	4.11	–	4.47	–	–	–
BC-15	19.26	145.97	160.25	–	–	–
BC-5	399.32	–	–	–	–	–
BC-17	–	3.97	–	–	–	–
BC-18	–	101.68	–	–	–	–
BC-13	–	–	409.85	–	–	–
BC-8	–	–	–	132.18	–	–
BC-3	–	–	–	94.38	–	–
BC-16	–	–	–	239.32	–	–
Range	–	–	–	–	4043.69	–
Coefficient of variation	–	–	–	–	1729.46	–
Maximum	–	–	–	–	300.24	–
Slope 6	–	–	–	–	–	737.15
Slope 1	–	–	–	–	–	596.44
Slope 7	–	–	–	–	–	245.37

Values are corresponded to the distance of each predictors from the centre of hypervolume niche of *C. wightii*

HHI: habitat heterogeneity indices

Table 7 Area ($\times 10^4$ km^2) of each habitat suitability class with studied bioclimatic and non-bioclimatic variables

Suitability classes	Current	2050	2070	2090	HHI	Land use	Slope	Soil
Optimal	8.67	7.73	5.5	10.16	17.34	104.45	0.066	40.62
Moderate	13.62	14.07	10.26	18.87	94.67	131.56	2.124	52.69
Marginal	13.65	18.11	9.58	24.55	120.01	39.89	3.83	199.35
Low	31.02	45.82	17.02	61.13	102.45	18.03	271.26	18.77
Total	66.96	85.73	42.36	114.71	334.47	293.93	277.28	311.43

Table 8 Area ($\times 10^4$ km^2) of each habitat suitability class with studied combinations of bioclimatic variables and non-bioclimatic variables (habitat heterogeneity indices + land use + slope + soil)

Suitability classes	Current + NBC	2050 + NBC	2070 + NBC	2090 + NBC
Optimal	153.93	137.79	124.72	114.27
Moderate	139.74	155.53	168.38	178.82
Marginal	3.57	3.06	2.75	2.85
Low	3.45	7.5	5.83	6.74
Total	300.69	303.88	301.68	302.68

the geographical distribution of different classes. The optimal area for this species with individual variables was recorded maximum with landuse (104.45×10^4 km^2), whereas the minimum was reported with slope and aspect variables (0.066×10^4 km^2). Among climatic variables, the highest area under the optimum suitability class was documented with a time frame of 2090. Maximum (131.56×10^4 km^2) and minimum (2.124×10^4 km^2) areas in the moderate class were recorded with HHI and slope variables, respectively (Table 7).

With soil quality factors, the maximum marginal area (199.35×10^4 km^2) was recorded. Maximum low suitability class was recorded with slope and aspect factors covering 271.26×10^4 km^2 area. HHI has the biggest total area (334.47×10^4 km^2), followed by soil (311.43×10^4 km^2), land use (293.93×10^4 km^2), and slope (277.28×10^4 km^2). Total area includes all suitability classes was lower

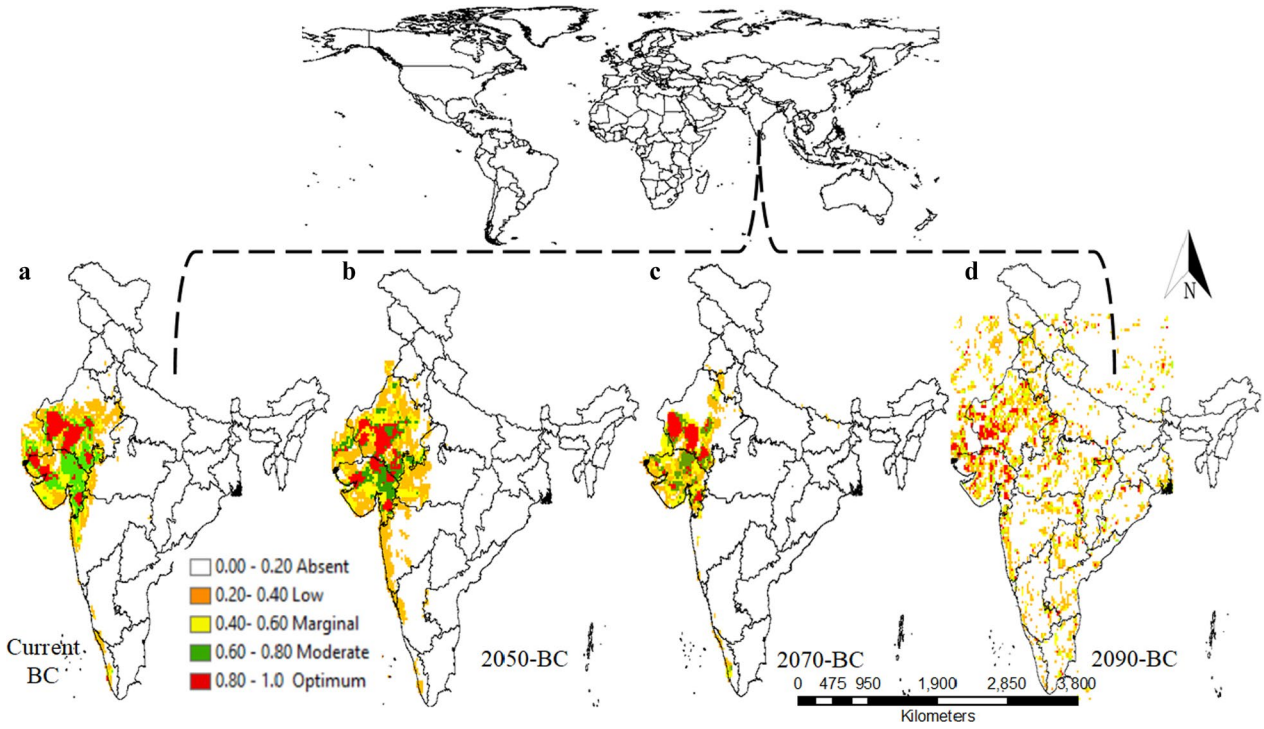

Fig. 14 Projected habitat suitability classes of *C. wightii* in India during various bioclimatic projection current (**a**), 2050 (**b**), 2070 (**c**) and 2090 (**d**)

with bioclimatic variables than with non-bioclimatic variables, with 2090 BC having the highest total area (114.71×10^4 km^2) and 2070 BC having the lowest (42.36×10^4 km^2) (Table 7). To limit the complexity and text length, we only summarize our results for the optimum and moderate classes. Details of specific sites under these suitability classes with different BC time frames and NBC are presented in Additional file 1.

Geographical locations of optimum and moderate classes within India: bioclimatic variables

With the current bioclimatic situation (Fig. 14a), the optimal region for this species is 8.67×10^4 km^2, which can be divided into four large patches extended at landforms includes hilly terrain, sandy hummocks, young alluvial plains and saline depressions, while moderate areas (13.62×10^4 km^2) dominantly located at Gujarat state. During the 2050 time frame, the optimum region will shrink in comparison to the existing scenario, and this suitability class will primarily located in Rajasthan state. We observed that greater lands in Gujarat state of optimum class were transformed to low suitability class (Fig. 14b). With the 2070 time frame, there was an overall drop of all suitability classes (Table 7). Optimal locations for this species seem to shift toward more western portions of the India (Fig. 14c). When compared to the previous two time periods, several places in Gujarat states would lose their optimal habitat. Moderate areas with this bioclimatic time frame will be located at hilly and young alluvial regions of Gujarat, and sandy areas of Rajasthan (Fig. 14c). In 2090, we had the most area in all classes compared to the preceding three time periods. However, we observed fragmentation of suitability classes over this time period (Fig. 14d). The optimum areas were identified in following states of India along with habitat types: Tamil Nadu (youngalluvial plain, hilly regions and river basin), Andhra Pradesh (YAP, hilly regions and river basin), Kerala and Chhattisgarh (hilly areas), Karnataka (YAP and hilly region), Telangana (YAP, hilly region, sandy beaches), Chhattisgarh (hilly region), Assam (YAP), Utter Pradesh, Maharashtra and Jharkhand, Odisha, Madhya Pradesh, Gujarat (YAP and hilly region), Rajasthan (sand dune, YAP and hilly regions). Details of specific locations are presented in Additional file 1.

Geographical locations of optimum and moderate classes within India: non-bioclimatic variables

Habitat heterogeneity index

Using this non-bioclimatic variable, our analysis found that the entire state of Rajasthan is covered by the optimum and moderate classes of this species (Fig. 15a). From North to West, areas with optimum class includes districts like Churu, Jhunjhunun, Bikaner, Barmer, Jaisalmer and Jodhpur. At Gujarat, area covers Koddha,

Zinzuwada, Hanjiyasar, Malia, Shiikarpur, Vavaniya, Nvalakhi. Moderate locations are identified at Kishangarh, Ajmer, Nasirabad, Jaitaran, Bar, Beawar, Bilara, Sojat, Marwar Junction, Falna, Sumerur, Siwana, Bagra, Diyodar, Tervada, Tharad, Palitana, Damnagar, Gariyadhar, Piyava, Jesar, Aurangabad, Jalna, Atpad, Pattadakal, Badami, Gajendragad, Rona, Holealur, Shalwadi, Nargund, Shalwadi, Hadagali, Navalgund, Annigeri, Mulgund, Sita, Chitradurga.

Soil

Soil variable suggested that areas of several districts of Rajasthan: Jaisalmer, Barmer, Jodhpur, Bikaner, Nagor, Sikar, Sirohi, Mount Abu, Jalore, Pali, Jhunjhunun, Churu, Ganganagar, Hanumangarh are optimum and moderately suitable for this species (Fig. 15b). Similarly, the entire coastal area of Gujarat, including Porbandar, Keshod, Madhavpur, Mangrol, Somnath, Kodinar, Talala, Una, Timbi, Kovaya, Putwa Bay, Dungar, Datardi, Longadi, Bhaguda, Talaja, Tharad, Bhavnagar, Dhotera, Anand, Borsad, Kava, Bhadkodara, Gandhar, Dahej, Dandi, Hazira, Dumas, Ubhrat, Navsari, Umargam, Dahanu are under optimum habitat for this species. Furthermore, several locations in Haryana, Punjab, New Delhi (Union Territory), Uttar Pradesh, West Bengal, and coastal portions of Andhra Pradesh and Kerala are ideal for this species.

Slope and aspect

With these geomorphological features, we observed that very few areas fall within the optimum and moderate categories. Nearby locations of Abasar (27° 50′ 34.80″ N and 74° 30′ 44.36″ E, elevation 319 m), Harasar (27° 50′ 20.10″ N and 74° 31′ 51.53″ E, elevation 317 m), Randhisar Pahari (27° 52′ 45.32″ N and 74° 31′ 22.80″ E, elevation 320 m), Nandiya Kalan (26° 44′ 46.79″ N and 73° 11′ 48.85″ E, elevation 321 m), Sutharo ki Dhani 26° 40′ 34.66″ N and 73° 12′ 51.89″ E, elevation 278 m), Bhagat ki Kothi (CAZRI, 26° 14′ 51.17″ N and 73° 00′ 57.59″ E, elevation 227 m), Vopari (25° 43′ 22.98″ N and 73° 47′ 16.11″ E, elevation 325 m), Sarwal (25° 43′ 14.88″ N and 80° 48′ 08.73″ E, elevation 108 m), Dahargaon (21° 43′ 22.84″ N and 78° 19′ 33.37″ E, elevation 691 m), Dharmaram (18° 27′ 14.74″ N and 78° 41′ 14.89″ E, elevation 450 m) provide the optimum conditions. With these characteristics, the majority of the Indian subcontinent was classified as having low appropriateness (Fig. 16a).

Land use

Using this variable, we identified that bigger portions of Rajasthan, including districts such as Jaisalmer, Barmer, Bikaner, Jodhpur, Pali, Sanchore, Jalore, Sirohi, Hanumangarh, Shri-Ganganagar, Sojat, Churu, Jhunjhunun, Ajmer, and Sikar, are best suited for this species. An elongated stretch including Nokha, Osian, Balotra, and Chautan localities, on the other hand, has moderate suitability for this species. The entire coastal parts of Gujarat, as well as some inland places such as Ahmedabad, Radhanpur, Anand, Deesa, Palanpur, and Surat, provide ideal habitat for this species. Some districts in Gujarat, like as Rajkot and Junagarh, are moderate for this species. The majority of Maharashtra state areas are classified as

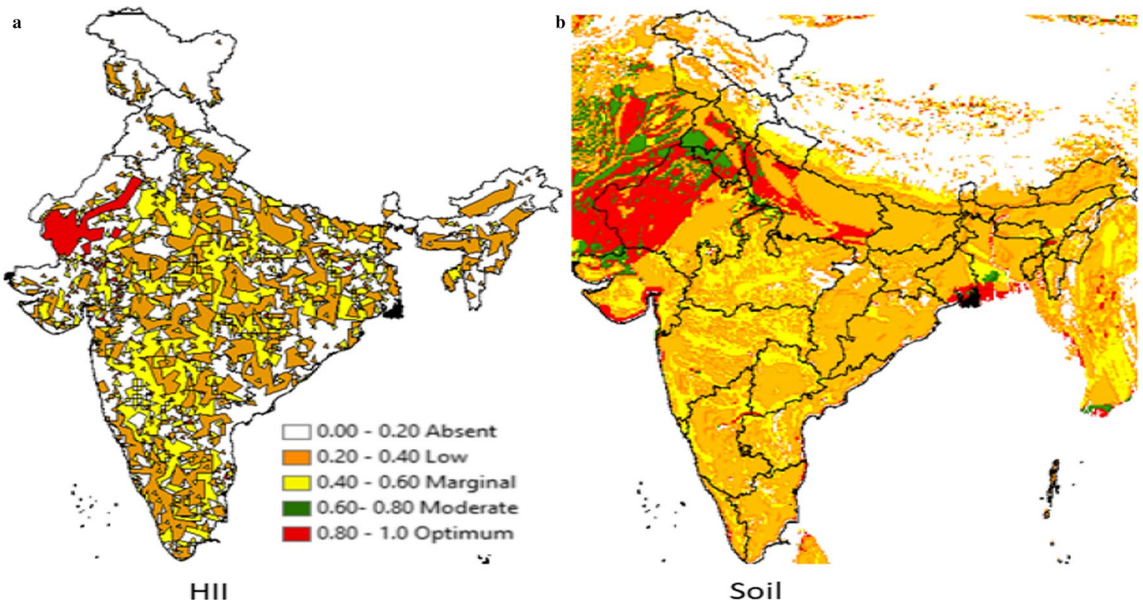

Fig. 15 Projected habitat suitability classes of *C. wightii* in India with non-bioclimatic variables HHI (**a**) and soil (**b**)

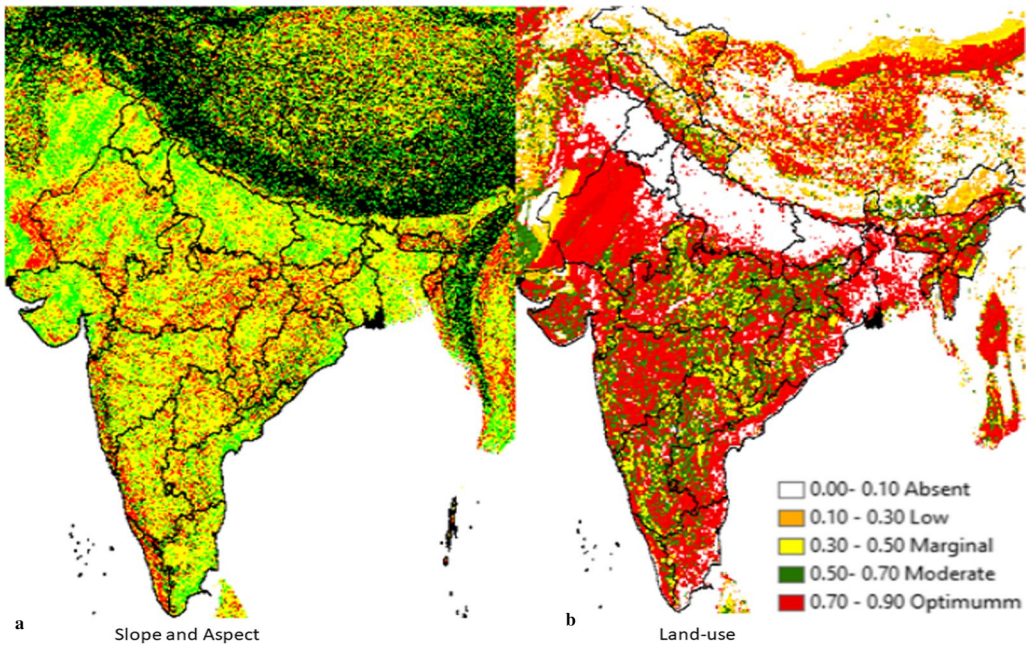

Fig. 16 Projected habitat suitability classes of *C. wightii* in India with non-bioclimatic variables slope (**a**) and land use (**b**)

Moderate (Fig. 16b). Southern coastal areas of Kerala, Karnataka, Tamil Nadu, Andhra Pradesh, and South-Eastern states like Telangana, Odisha, and West Bengal are also ideal habitat. Similarly, a few districts in Uttar Pradesh, such as Varanasi, Etowah, Mainpuri, Prayagraj, Jhansi, and Rewa, are moderate for this species. Among the hilly places, Dharmshala, Manali, Shimla, Dehradun, Nanital, and Haldwani have shown the best suitability.

With a combined data set of bioclimatic and non-bioclimatic variables, we found that the area under optimal and moderate classes was greater than the area under marginal and low classes (Table 8). The highest area under optimal class was recorded with the combination of NBC with the current bioclimatic scenario, followed by 2050, and the least with 2090, while the contrary tendency was observed for the moderate class, which was greatest with 2090 and least with the current scenario. This inverse trend equalizes the total area under all BC and NBC combinations that ranged from 300.69 to 302.68 (Fig. 17a–d).

Our analysis of the current combined scenario revealed higher optimal areas in western states (including

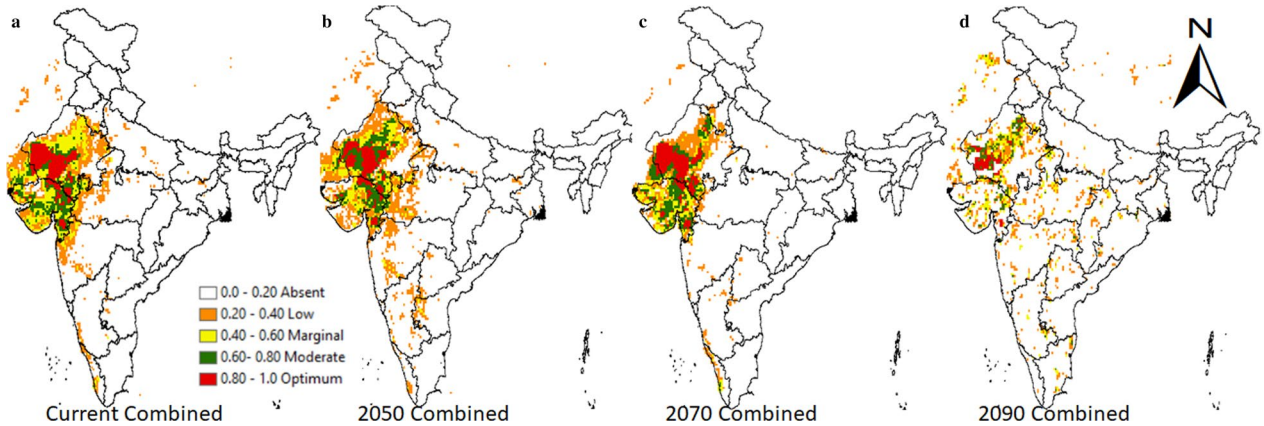

Fig. 17 Projected habitat suitability classes of *C. wightii* in India with combinations of bioclimatic and non-bioclimatic variables (habitat heterogeneity indices + land use + slope + soil), current combination (**a**), 2050 combination (**b**), 2070 combination (**c**) and 2090 combination (**d**)

Rajasthan and parts of Gujarat), Western Ghat (Karnataka, Kerala), and Eastern Ghat (Tamil Nadu, Andhra Pradesh, and Telangana), eastern region (Odessa and West Bangel), and some northern regions (including Himachal Pradesh, Uttarakhand). As climatic time periods progressed, we saw a decrease in the intensity of this class (Fig. 17a–d). Maximum moderate areas were envisioned with 2090, which covered various states in central India as well as northern and western sections of the country, notably Gujarat state.

Percent changes in mean habitat suitability

Results of percent changes in mean habitat suitability between two bioclimatic time periods are presented in Additional file 1: Fig. S4. There was a reduction in optimal suitability class between time frames current–2050 (−10.84%), current–2070 (36.56%), and 2050–2070 (−28.85%). As a result, the optimum suited zones for this species will shrink between now and 2070. However, when we examined our data from now to 2090 and 2070–2090, we found that this class increased by 17.19% and 84.73%, respectively.

Our findings also demonstrated that the overall percent reduction area for all suitability classes decreased between current–2070 and 2050–2070, while we recorded an overall increase in area for all classes between the bioclimatic time frames of current–2090, 2050–2090, and 2070–2090 (Additional file 1: Fig. S4). The higher percent growth in area of this species across all classes between 2070 and 2090 (83.92 to 259.17 percent) demonstrates the resilience acquired by this species over specific bioclimatic time frames.

Results of the percent change in suitability class with combinations of bioclimatic variables and non-bioclimatic variables (HHI + land use + slope + soil) are depicted in Additional file 1: Fig. S5. We observed an overall decrease in the area of the optimum and marginal classes with all types of combinations, except for the marginal class with 2070 + NBC to 2090 + NBC. Maximum percent decrease (25.76%) was obtained with Current + NBC to 2090 + NBC. In contrast to the optimum class, all types of pairings resulted in an overall increase in the moderate suitability class. Maximum (27.97%) recorded with Current + NBC to 2090 + NBC. Decreasing trends for the low suitability class were observed between 2050 + NBC and 2070 + NBC (−22.27%) and 2050 + NBC and 2090 + NBC (−10.13%), whereas increasing trends for this class were observed between current + NBC and 2050 + NBC (117.39%), current + NBC to 2070 + NBC (68.99%), current + NBC to 2090 + NBC (95.36%), and 2070 + NBC to 20 (15.61%). Percent area change (total) likewise demonstrated similar tendencies, with 2050 + NBC to 2070 + NBC (−0.72%) and 2050 + NBC to 2090 + NBC (−0.39%).

Changes in core distribution centres

We employ Maxent output in conjunction with ArcMap's SDM Tool Box to determine the centroid of this species, specifically under the optimum class for all bioclimatic time-frame projections (Additional file 1: Fig. S6). Its ideal centroid is currently located in Jalor district of Rajasthan state, but it will be relocated to Tharad district of Gujarat state 111.11 km distant by 2050. Between 2050 and 2070, the centre will move 102 km further from Tharad in Rajasthan, while its centroid migrated 83 km from 2070 to 2090 and is now located in Barmer, Rajasthan at 72° 28′ E and 26° 15′ N between Balotra and Patodi areas.

Niche overlap

The amount of niche retained by this species under various projections was visualized using niche overlap analysis. To depict the ecological niche overlap, Schoener's *D* (which evaluates the consistency of niche overlap per pair) and Hellinger's-based *I* (which represents the degree of overlap of the geographical distribution) values were used. The values of Schoener's *D* and Hellinger's *I* range from 0 to 1, with values closer to 0 indicating a low degree of niche overlap and values closer to 1 indicating a high degree of niche overlap. Tables 9 and 10 show the values of the Schoener's *D* and Hellinger's *I* indices. Highest *D* (0.74) and *I* (0.94) values were recorded between current and 2070 BC, while the lowest values of both these indices (0.33 and 0.54) were recorded between Soil-2050 as well as Soil-2070. Both *D* and *I* values are nearly identical for the combined data set (Table 11).

Automated conservation assessments

Table 12 depicts the current state of *C. wightii* as well as the impact of niche modelling on EOO and AOO using the Maxent algorithm output. EOO and AOO were 1,170,653 and 480 km^2, respectively, with our actual spatially thinned population. However, with the predicted current BC, the EOO was lowered to 909,237 km^2, while the AOO (1540 km^2) increased. Among BC and NBC variables, the highest EOO (6,007,288 km^2) was recorded with slope and aspect variable, similarly the highest AOO (5244 km^2) was recorded with HHI variable. With projected variables, lowest EOO (894,197 km^2) and AOO (744 km^2) were recorded with 2070 and 2090 time frames, respectively. We found a substantial positive linear association between spatially thinned population size and AOO (Additional file 1: Fig. S7), which can be interpreted as follows: $Y = 3.998\ X$, $R^2 = 0.99$.

Table 9 Niche overlap Schoener's *D* values between various bioclimatic and non-bioclimatic variables (individual)

	2050	2070	2090	Current	HHI	Land use	Slope
Soil	0.33	0.33	0.39	0.34	0.44	0.69	0.47
2050	–	0.65	0.54	0.74	0.50	0.45	0.65
2070	–	–	0.50	0.75	0.42	0.43	0.65
2090	–	–	–	0.53	0.57	0.54	0.73
Current	–	–	–	–	0.49	0.43	0.64
HHI	–	–	–	–	–	0.70	0.65
Land use	–	–	–	–	–	–	0.49

Table 10 Niche overlap Hellinger's *I* values between various bioclimatic and non-bioclimatic variables (individual)

	2050	2070	2090	Current	HHI	Land use	Slope
Soil	0.57	0.55	0.62	0.58	0.66	0.89	0.65
2050	–	0.90	0.76	0.93	0.74	0.70	0.77
2070	–	–	0.74	0.94	0.71	0.67	0.77
2090	–	–	–	0.77	0.79	0.78	0.82
Current	–	–	–	–	0.76	0.69	0.77
HHI	–	–	–	–	–	0.89	0.81
Land use	–	–	–	–	–	–	0.68

Table 11 Niche overlap Schoener's *D* and Hellinger's *I* values between various bioclimatic and non-bioclimatic variables for combined data set

Bioclimatic time frames	*D* index (combined)			*I* index (combined)		
	2050	2070	2090	2050	2070	2090
Current	0.98	0.99	0.99	1.0	1.0	1.0
2050	–	0.99	0.99	–	1.0	1.0
2070	–	–	0.98	–	–	1.0

Table 12 Population dynamics of *C. wightii* and IUCN evaluation of extent of occurrence and area of occupancy calculated for both real data set and projected data set with BC and NBC variables

Data set types	Population size of *C. wightii* up to moderate suitability class (before spatial thinning)	Population size after spatially thinning	EOO (km^2)	AOO (km^2)
Real occurrences	144	130	1,170,653	480
Projected current-BC	844	385	909,237	1540
Projected 2050-BC	818	389	1,291,939	1556
Projected 2070-BC	607	290	894,197	1160
Projected 2090-BC	261	186	3,938,063	744
Projected HHI	2589	1311	4,506,402	5244
Projected slope	325	276	6,007,288	1104
Projected land use	34,259	468	4,535,803	1872
Projected soil	13,547	343	4,249,718	1372

Discussion

Slow growth, poor seed establishment and germination, lack of cultivation, overharvesting for religious and household use (as fuel by rural people), and improper tapping for its gum resin by pharmaceutical enterprises have likely contributed to *C. wightii* extinction (Parmer 2003; Soni 2010; Jain and Nadgauda 2013; Kulhari et al. 2014; Singhal et al. 2014; Kumar and Kulloli 2017; Saini et al. 2018; Choudhary et al. 2021; Brindavanam et al. 2022). In India, studies identified province based source of variation in reproductive (Gupta et al. 1996; Yadava et al. 1999; Prakash et al. 2000; Kasera and Prakash 2005; Haque et al. 2009, Yadava 2011; Bishoni et al. 2018; Brindavanam et al. 2022), phenological (Singhal et al. 2014; Samanta et al. 2016) and morphological (Sinha et al. 2012; Tripathi et al. 2016) traits of *C. wightii*. Phytosociological exploration (Reddy et al. 2012; Tomar 2013, 2021; Kulloli et al. 2016; Kumar and Kulloli 2017) of this species also revealed the significant impacts of land use and landform types on the population density of this species. Soil variables (texture, electric conductivity, pH, and available phosphorus) in relation to density and diversity of this species have been documented by Soni (2010), Kulhari et al. (2012) and Kulloli et al. (2016). However, cause-and-effect relationships between predictors and different traits of this species are very limited.

Our research filled scientific gaps concerning *C. wightii* national extent and area of occupancy. This study also emphasized the significance of bioclimatic and non-bioclimatic predictors on this species' current and future fate. Previous phytosociological observations documented its ecological characteristics primarily in the western hot arid and semi-arid parts of the country; however, our modelling approach revealed additional potential habitat for this species, including regions in both the southern and eastern halves of the country. In vitro research suggests an improved methodology for enhancing natural regeneration, specifically preferring plantation with stem cuttings over seeds (Soni 2010). Environmental conditions following planting, on the other hand, are critical to the success of rehabilitation, restoration, and reclamation efforts.

Population Viability Analysis (PVA) is able to predict a species' susceptibility in terms of the number of years it has left to live under the current environmental conditions, which can be used to estimate the likely remaining life span for a vulnerable plant species under the current environmental conditions. However, this kind of analysis calls for the gathering of density data over a long period of time (more than 20 years, Mathur 2014a). In the case of *C. wightii*, the majority of ecological parameters are collected from single field-based inventories, whereas other phenological, reproductive, and morphological traits of this species were obtained through pure field-based investigation or through the use of some biotechnological approaches, and the results were interpreted based on their collection sites (provinces). However, as was already mentioned, PVA analysis needs a set of repetitive temporal data to be able to predict whether a species will succeed or fail in its environment. For *C. wightii*, this type of data is lacking. Therefore, the most appropriate scientific approach for predicting the future of this species as well as the role of various predictors is evidence-based conservation inventories, such as modelling of *C. wightii* spatial suitability in relation to different climate change scenarios and with bottom-up (plant community dynamics, slope, and land use type) and top-down (soil qualities) factors.

The earth's temperature has risen over the past 100 years, and new changes in precipitation patterns are anticipated in the future. These changes could directly or indirectly affect how species are distributed (Thakur et al. 2022). The species' phenological and metabolic activities may be dynamically affected by changes in temperature and precipitation. Additionally, anthropogenic activity and climate change may accelerate the spread of pathogens, invasive species, and pests, preventing their regrowth and establishment in their natural habitats. The impact of bioclimatic variables may be influenced by regional biophysical features depending on slope and other geographical factors (Austin and van Niel 2011). As shown in the current study, understanding the roles of the soil, plant community, slope, and land use pattern is crucial for enhancing distribution modelling.

The loss of habitat, deforestation, degradation of the forest, overexploitation, climate change, and land degradation are just a few of the serious threats that native Indian species must contend with (Rajpoot et al. 2020). All of India's territory, including Himachal Pradesh and Uttarakhand in the north, Jharkhand and portions of Chhattisgarh in the east, Odisha in the eastern coastal regions, and Karnataka and Andhra Pradesh in the south, has been studied for climate suitability (Sen et al. 2016a, b; Ray et al. 2018; Sharma et al. 2018; Bhandari et al. 2020). Maxent modelling was employed by researchers from the Indian subcontinent to ascertain the significance of bioclimatic variables for the distribution of *Myristica dactyloides, M. fatua, M. malabarica, Knema attenuate*, and *Gymnacranthera canarica* (Priti et al. 2016), *Parthenium hysterophorus* (Ahmad et al. 2019), *Aristolochia indica* (Sarma et al. 2018; Tiwari et al. 2022) and *Clerodendrum infortunatum* (Purohit and Rawat 2022). On the other hand, similar kinds of scientific inventories are incredibly rare for plant species found in India's hot, arid, and semi-arid regions.

For predicting potential distribution under various climatic conditions, the *C. wightii* Maxent model produced all AUC values greater than 0.940, which was consistent with earlier studies on other economically and medicinally important species (Remya et al. 2015; Yi et al. 2016; Adhikari et al. 2018; Sharma et al. 2018). Non-bioclimatic parameters, with the exception of terrain slope and aspect, decreased the accuracy of our model. Additionally, Maxent accuracy was the lowest across all combinations of bioclimatic and non-bioclimatic variables (AUC = 0.75 to 0.78). This suggested that predictions for this species would be more accurate if they were based on either bioclimatic or non-bioclimatic variables; however, if we wanted to combine these two predictors, our model quality would be primarily limited by community members and habitat types, such as forest, grassland, or shrublands. Even with a model that accurately fits the data, a low AUC value may suggest poor discrimination between presences and absences, according to West et al. (2016). The number of predictors may also be related to this decline in AUC values (Li et al. 2020). Because we had fewer variables (non-bioclimatic) to examine than bioclimatic variable numbers, this was true for our data set. The current study is the first to determine the Maxent model's accuracy at three distinct levels, including the sum of individual bioclimatic and non-bioclimatic variables as well as their combinations. Therefore, our study can also add new methodological information for ENM analysis of plant species based on such findings.

In arid grazing lands in India, we previously evaluated the impact of *Prosopis juliflora* invasion on the population dynamics of *C. wightii*. We unearthed that *C. wightii* density decreased as *P. juliflora* density increased (Kumar and Mathur 2014). In order to further understand the behaviours of such variables, community types and species-specific associations ENM modelling for this species would be useful.

Our predictions indicated that, with the exception of 2070, the distribution of *C. wightii* in potentially suitable climates would increase in the order of 2090 > 2050 ≈ current, indicating that more suitable habitats are available for increasing the current population of *C. wightii* through artificial cultivation and will be available for future bioclimatic projections of 2050 and 2090. These results were in line with earlier research that predicted that some locations would experience an improvement in the habitat suitability of plant species as a result of climate change (Gupta et al. 2023).

With our non-bioclimatic variables, we found more inter-variable variation for the area under the various classes. In the following order, the highest area under the optimal class was noted: and land use > soil quality > HHI > slope. The tendency was slightly different for moderate suitability, with land use coming before HHI, soil, and slope. Additionally, the total area (which includes all classes) shows various perspectives for HHI, land use, soil property, and slope and aspect. The biology of this species' reproduction can also be used to evaluate the aforementioned realization. In general, apomictic species can occupy a wider range of habitats than sexual and self-incompatible species because they are more independent of pollinator services (Horandl et al. 2018). The research by Bishoni et al. (2018) found that genetic variation trends in *C. wightii* were also correlated with population reproductive behaviour rather than geographic location. In contrast to the sexual population of Gujarat, particularly that of the Kutchh, Dwarka, and Jamnagar areas, which exhibited the highest genetic variability, the apomictic Rajasthan populations had somewhat lower genetic diversity. They came to the conclusion from their RAPD analysis that these particular regions can be regarded as the original *C. wightii* distribution areas from which the species was spread to the other regions of Gujarat and Rajasthan. This species may have become apomictic due to the prevailing unfavourable environmental conditions found in the newly acclimatized areas. Our findings suggested that less suitable areas might also be able to support this species, but some human intervention is needed. The slope and aspect modification, community members, soil property (excess salt and rooting conditions), and finally selection of land uses (GRS that denote percent share of grassland/scrub/woodland) can all be done in accordance with our best-class values for non-bioclimatic variables (Table 7).

Our Maxent modelling with the fusion of bioclimatic and non-bioclimatic variables revealed a clear trend regarding the area under different habitat suitability classes. This trend implied that with such predictors, the optimum areas for this species will decrease as we advance with climatic time frame (current, 2050, 2070, and 2090), while the opposite trend was observed for moderate suitability. In contrast, the overall area for all classes showed roughly equal areas for all BC and NBC combinations. This finding contradicts the findings of Wei et al. (2018), who associate the lack of their Maxent modelling tendency for *Carthamus tinctorius* with human intervention (Gonzalez-Moreno et al. 2015), environmental factor selection (Radosavljevic and Anderson 2014), and uncertainties associated with IPCC global climate models (Mcsweeney et al. 2015).

VIP values of various water availability parameters such as AnPr, PrWeM, PrDM, PrS, PrWeQ, PrDQ, PrWaQ, and PrCQ indicate their controls on *C. wightii* habitat suitability during the current, 2050, and 2070 climatic time frames. In contrast, with 2090 projection, energy variables such as isothermality and MeTWeQ will be the

governing factors for this species (Table 2). Our findings using current and 2070 bioclimatic projections revealed that, despite having the highest importance value, PrCQ can only help *C. wightii* in the low suitability class (Figs. 4a and 6a). As a result, we can conclude that winter precipitation (extreme colder conditions) hampered the survival of this species during these time frames. Mondal et al. (2022) advocate similar findings for ENM analysis of other plant species from the Indian region.

According to Goncalves et al. (2014), the seasonality of precipitation (i.e. the total precipitation of each month and their standard deviation—BC-15) provides a measure of the amount of soil water that is available for plant growth. This factor was found to be significant during the current, 2050, and 2070 climate projections and was more suited for *C. wightii* at a peak between 140 and 160 mm. Additionally, in future bioclimatic projections, precipitation in the warmest quarter (based on data on the average temperature and total precipitation for each month), in driest quarter (data of total precipitation for each month, 2050), in wettest month (total precipitation for each month, 2070), and in wettest quarter (2090) also suggested the significance of rainfall or water availability for the habitat suitability of this species.

Abundant rainfall leads to a significant increase in soil water content near the plant, providing an excellent growth environment for *C. wightii*. However, if the rainfall is too much (200 mm), the waterlogging stress will lead to the closure of stomata, the decrease of photosynthetic capacity and the increase of respiratory energy consumption, which is not conducive to the accumulation of organic matter. *C. wightii* growth pattern, leaf production, canopy cover and oleo-gum production quality and yields were significantly altered with temporal/seasonal changes (Samanta et al. 2016). Highest gum production was reported with high precipitation period, i.e. September and lowest during water stress conditions (April to May). From this species, the production of economically important gum was physiologically related with transpiration rate/demand. Observed highest quantity when transpiration was low (rainy season, September) and produce lower resin when extreme drought stress occurs during late summer. Thus, for this deciduous species, extreme water deficits can ultimately lead to a collapse of the carbon allocation to secondary metabolism while, favourable soil moisture and plant water status critically enhanced physiological function which resulted in higher energy status, sap flow and turgor to enable gum oozing (Samanta et al. 2012). Among the energy variables, we noticed that the maximum temperature of the warmest month (38–42 °C) during current climatic conditions and the mean temperature of the wettest quarter (10 and 15 °C) and isothermality (how large the day-to-night temperature oscillate relative to the summer to winter (annual) oscillations (0.25 to 0.30) during 2090 will affect this species' habitat.

In general, plant growth is hampered by salinity because it inhibits water uptake. Moderate salinity has an effect on growth and yield; high salinity levels may kill the plant. Sodicity causes sodium toxicity and has an impact on soil structure, resulting in a massive or coarse columnar structure with low permeability. Conditions indicated by saline and sodic phases may affect crop growth and yields in addition to soil salinity and sodicity. Furthermore, effective soil depth (cm) and effective soil volume (vol. %) are two rooting conditions that are affected by the presence of gravel and stoniness. The presence of a soil phase may affect rooting conditions by limiting the effective rooting depth or decreasing the effective volume accessible for root penetration. Rooting conditions address the various relationships between rooting zone soil conditions and crop growth. Rooting condition evaluation is important because it provides valuable information on the adequacy of foothold (i.e. sufficient soil depth for the crop to anchor), available soil volume and penetrability of the soil for roots to extract nutrients, space for root and tuber crops to expand and economic yield in the soil, and the absence of shrinking and swelling properties affecting root and tuber crops.

In the present study, soil variables like excess salt and rooting conditions, revealed that they only support this species up to the moderate class. Our earlier empirical study (Kulloli et al. 2016) between soil factor and ecological dominance of this species demonstrated that neutral soil reaction (neither acidity nor sodicity/salinity) benefited this species. Furthermore, potassium levels in the mid-range (200–300 kg/ha) were shown to be most beneficial to *C. wightii* density and health. The current study also demonstrated that textural habitat heterogeneity characteristics, such as range coefficient of variance and maximum, could support this species at an optimal level (Fig. 10a–c). Furthermore, slope and aspect, as well as land use variables, promote this species in a comparable way. In conclusion, the coefficient of variation obscured the effects of bioclimatic variables across all time frames when BC+NBC were combined, and these findings point to the much greater influence of dispersion of vegetation indices.

We modelled the distribution of *C. wightii* to explain its niche stability, proportion of native niche and niche expansion, and the likely environmental factors associated with such distribution in both native (western India) and exotic (north-east, central part of India, as well as northern and eastern Ghat). In order to simulate both its fundamental niche (defined as a species' capacity to persist and procreate in a wider range of environments when

not competing with other species; Franklin 2009) and its realized niche (when it is in the presence of other interacting species; Booth 2017), we examined the impact of niche modelling on its EOO and AOO. In order to evaluate the RET in India and Egypt under climate change, Adhikari et al. (2018) and Kaky and Giblbert (2019) have previously argued for the inclusion of species distribution models and IUCN Red List criteria.

To the best of our knowledge, this is the first study into how *C. wightii* niches overlap. In comparison to non-bioclimatic variables, bioclimatic variables had better consistency of niche overlap (*D*) and degree of overlap (*I*). Additionally, it was the smallest variable among bioclimatic and non-bioclimatic factors. *D* and *I* values were nearly identical for the combined bioclimatic and non-bioclimatic variables, though. This finding demonstrated that this species has two distinct types of tendencies for various predictor types. For instance, compared to non-bioclimatic predictors, it can share more among bioclimatic forecasters. But when both of these predictors are equally potent, this species changes its propensity to retain its niche and displays full niche overlap for better survival. Such results have already been reported for *Paeonia mairei* (Chen et al. 2020), and *Betula utilis* (Hamid et al. 2019).

The Red List Categories and its associated five criteria developed by the International Union for Conservation of Nature (IUCN) provides an authoritative and comprehensive methodology to assess the conservation status of species. Red List criterion B, which principally uses distribution data, is the most widely used to assess conservation status, particularly of plant species. The Criterion B is suitable for estimating conservation status even when the distribution of a taxon is only known from georeferenced herbarium or museum collections and with limited information on local threats and potential continuing decline, and it plays a prominent role in describing global trends in extinction risk. Criterion B involves two sub-criteria (B1 and B2), which reflect two different kinds of geographic range size estimates [sub-criterion B1 is based on extent of occurrence (EOO) while B2 is based on area of occupancy (AOO)].

Extent of occurrence (EOO) is defined as "*the area contained within the shortest continuous imaginary boundary that can be drawn to encompass all the known, inferred or projected sites of present occurrence of a taxon, excluding cases of vagrancy*". EOO is generally measured by a minimum convex polygon, or convex hull, defined as "the smallest polygon in which no internal angle exceeds 180° and which contains all the sites of occurrence (IUCN 2010)." AOO differs from EOO as it reflects the fact that a taxon will not usually occur all over its EOO, that is, there will be areas where the taxon is absent, including (unsuitable areas). The AOO will be a function of the scale or grid cell size at which it is measured, and which should reflect relevant biological aspects of the taxon (i.e. AOO = number of occupied cells × area of an individual cell). The intent of EOO is to 'measure the degree to which risks from threatening factors are spread spatially across the taxon's geographic distribution' (IUCN 2022), while the primary intent of AOO is 'as a measure of the "insurance effect", whereby taxa that occur within many patches or large patches across a landscape or seascape are "insured" against risks from spatially explicit threats (Guillera-Arroita et al. 2015). With B1a + B2a, we can classify this species as least concern or near threatened based on our expected EOO and AOO. Our findings contrast those of Reddy et al. (2012) and Kumar and Kulloli (2017), both of whom conducted research in Rajasthan State. However, our results are supported with study of Khan et al. (2022) who calculated higher EOO and AOO for *Pinus gerardiana* with bioclimatic and non-bioclimatic gradients at South Asia (India, Pakistan and China). Our anticipated range and area of occurrence reflect the possibility of many areas in India where this species can be planted and grown.

The current study confirms the findings of previous phytosociological investigations by Kumar and Shanker (1982), Dixit and Rao (2000), Maheshwari (2010), Mertia et al. (2010), Reddy et al. (2012), Kulloli et al. (2016), Kumar and Kulloli (2017), and Tomar et al. (2021). The majority of such research identified rocky substratum (shallow, gravelly, infertile soils, mountainous terrains) as its preferred niche in both protected and non-protected settings. However, in this study, in addition to rocky sites, our potential locations also include habitats like sand dunes, sandy plains, young alluvial plains, salty areas, and so on.

According to agro-climatic classifications of Rajasthan and Gujarat (Mall et al. 2016; Mathur and Sundaramoorthy 2019), the semi-arid eastern plain (500–700 mm), transitional plain of the Luni river basin (300–500 mm), and hyper-arid partial irrigated zone (100–350 mm) in Rajasthan are the most suitable environments for this species. Similar regions in Gujarat state include semi-arid ones (1000–1500 mm heavy black clayey soils) and arid and semi-arid ones (250–500 mm sandy loam to sandy soil). This species does not do well in Rajasthan's irrigated northwest plains (100–350 mm), internal drainage dry zone (300–500 mm), or flood-prone eastern plain (500–700 mm).

We noticed a decline in optimal regions in Gujarat state by the year 2050. Additionally, with a climatic time frame of 2070, we observed a shift in the optimal class toward the western half of India, particularly in the districts of Jaisalmer and Barmer of Rajasthan. We found that most

regions of the nation were optimum suited for this species during the 2090 climate time frame. According to non-bioclimatic factors like soil, this species can be found in Rajasthan, Gujarat, as well as several other states like Haryana, Punjab, New Delhi, Uttar Pradesh, West Bengal, and coastal areas of Andhra Pradesh and Kerala. Similar to how HHI variables indicate that Rajasthan and Gujarat are the most preferred locations, land use factors indicate that this species may also prefer other states like Uttar Pradesh and Himachal Pradesh.

Conclusion

In this study, potential *C. wightii* distribution areas were assessed in relation to present, and projected bioclimatic conditions as well as non-bioclimatic factors. The ENM model's accuracy increased with bioclimatic variables, decreased with non-bioclimatic variables, and was lowest when both bioclimatic and non-bioclimatic variables were present. Within these predictors, we also pinpointed the most crucial variables influencing habitat types. Based on the calculated area under various suitability classes, we can say that *C. wightii*'s potentially suitable climatic distribution under the optimum and moderate classes would increase under all future bioclimate scenarios (2090 > 2050 $\approx$ current), with the exception of 2070, showing that there are more suitable habitats available for *C. wightii* artificial cultivation and will be available for future bioclimatic projections of 2050 and 2090. Additionally, we simulated its dispersal in both its native (western India) and exotic environments (Northeast, Central Part of India as well as northern and eastern Ghat). Our niche hypervolume analysis reveals that this species has two distinct types of proclivities in relation to different predictors. It may be shared more among bioclimatic forecasters than among non-bioclimatic forecasters, for example. However, when both of these predictors are equally powerful, this species shifts its proclivity for niche retention and exhibits complete niche overlap for enhanced survival. This species also prefers landforms other than rocky habitats, such as sand dunes, sandy plains, young alluvial plains, saline locations, and so on. Based on our findings, we can conclude that the studied BC and NBC predictors will positively support suitable habitats for this species, and that this species will be more resilient to the examined predictors. However, as we can see in the current situation, human activities will ultimately determine how well the new habitats support this species in the future.

We also agreed to take a cautious approach because we only used bioclimatic data from SSP-4.5 (greenhouse gas emissions are similar to current time frame) to model this species' ecological niche. We would be better able to grasp this species' ENM if the assessment used additional SSPs, such as 2.6, 6.0, and 8.5 (which, respectively, indicate very little to greatest GHG emission). Future research may also take into account the application of numerous different machine learning approaches, including random forest, support vector machine, artificial neural networks, and their ensemble methodology.

Abbreviations

AMT	Annual mean temperature
Iso	Isothermality (BC-2/BC-7) (×100)
MaTWaM	Max temperature of warmest month
TAR	Temperature annual range (BC-5 – BC-6)
MeTDQ	Mean temperature of driest quarter
MeTCQ	Mean temperature of coldest quarter
PWeM	Precipitation of wettest month
PS	Precipitation seasonality (coefficient of variation)
PDQ	Precipitation of driest quarter
PCQ	Precipitation of coldest quarter
MeDR	Mean diurnal range (mean of monthly (max temp – min temp))
TS	Temperature seasonality (standard deviation × 100)
MiTCM	Min temperature of coldest month
MeTWeQ	Mean temperature of wettest quarter
MeTWaQ	Mean temperature of warmest quarter
AP	Annual precipitation
PDM	Precipitation of driest month
PWeQ	Precipitation of wettest quarter
PWaQ	Precipitation of warmest quarter
AOO	Area of occupancy
ANN	Artificial neural network
CART	Classification trees
EOO	Extent of occurrence
GLM	Generalized linear models
GUI	Graphical user interface
Maxent	Maximum entropy
RF	Random forest
ROC	Receiver operating characteristic
AUC	Area under the receiver operating curve
BC	Bioclimatic variables
NBC	Non-bioclimatic variables
ENM	Ecological niche model
GAM	Generalized additive models
GARP	Genetic algorithm
MD	Mahalanobis distances
MARS	Multivariate adaptive regression splines
RET	Rare endangered and threatened
YAP	Young alluvial plain

Supplementary Information

The online version contains supplementary material available at https://doi.org/10.1186/s13717-023-00423-2.

Additional file 1. Provides information's on figures and tables related to correlation analysis, per cent change in area, centroid shift, relationship between population size and area and information on spatial extent of this species.

Acknowledgements

Senior author is thankful to the Director, ICAR-CAZRI for giving approval to him for attending training on R-Programming that enhanced his working capacity using ENM modelling techniques. Miss Preet Mathur (Jodhpur Institute of Engineering and Technology, Jodhpur, India) and Mr. Harshit Purohit (Neal Analytics, Pune, Maharashtra, India) are thankful to their Director for extending their academic help.

Author contributions
Senior author conceptualized the chapter theme and interpretation of output of various machine learning techniques. Both co-authors prepared various types of language codes in python, Java and in R scripts and convert the various file format from ASCII to KML, Raster, dbf, CSV, etc., for softwares like QGIS 3.10.0; Wallace; DIVA-GIS version 7.5; MaxEnt 3.4.1 software; SDM toolbox; Map Comparison Kit; ENMTools and Ntbox. All authors read and approved the final manuscript.

Funding
Not available.

Availability of data and materials
The data sets used and/or analysed during the current study are available from the corresponding author on reasonable request.

Declarations

Ethics approval and consent to participate
Not applicable.

Consent for publication
Not applicable.

Competing interests
The authors declare that they have no competing interests.

Author details
[1]ICAR-Central Arid Zone Research Institute, Jodhpur 342 003, India. [2]Jodhpur Institute of Engineering and Technology, Jodhpur, India. [3]Neal Analytics, Pune, Maharashtra, India.

Received: 1 July 2022 Accepted: 6 February 2023
Published online: 27 February 2023

References

Abolmaali SMR, Tarkesh M, Hossein B (2017) MaxEnt modelling for predicting suitable habitats and identifying the effects of climate change on a threatened species, *Daphne mucronata*, in central Iran. Ecol Inform 43:116–123. https://doi.org/10.1016/j.ecoinf.2017.10.002

Adhikari D, Reshi DBK, Samant SS, Chettri A, Upadhaya K, Shah MA, Singh PP, Tiwary R, Majumdar K, Pradhan A, Thakur ML, Salam N, Zahoor Z, Mir MH, Kaloo ZA, Barik SK (2018) Inventory and characterization of new populations through ecological niche modelling improve threat assessment. Curr Sci 114(3):519–531

Ahmad R, Khuroo AA, Hamid M, Charles B, Rashid I (2019) Predicting invasion potential and niche dynamics of *Parthenium hysterophorus* (Congress grass) in India under projected climate change. Biodivers Conserv 28:2319–2344. https://doi.org/10.1007/s10531-019-01775-y

Austin MP, van Niel KP (2011) Improving species distribution models for climate change studies: variable selection and scale. J Biogeogr 38:1–8

Barve DM, Mehta AR (1993) Clonal propagation of mature elite trees of *Commiphora wightii*. Plant Cell Tissue Organ Cult 35(3):237–244. https://doi.org/10.1007/BF00037276

Behera MD, Roy PS (2019) Pattern of distribution of angiosperm plant richness along latitudinal and longitudinal gradients of India. Biodivers Conserv 28:2035–2048. https://doi.org/10.1007/s10531-019-01772-1

Behera MD, Behera SK, Sharma S (2019) Recent advances in biodiversity and climate change studies in India. Biodivers Conserv 28:1943–1951. https://doi.org/10.1007/s10531-019-01781-0

Bhandari MS, Meena RK, Shankhwar R, Shekhar C, Saxena J, Kant R, Pandey VV, Barthwal S, Pandey S, Chandra G, Ginwa HS (2020) Prediction mapping through Maxent modeling paves the way for the conservation of *Rhododendron arboreum* in Uttarakhand Himalayas. J Indian Soc Remote Sens 48:411–422

Bishoni AK, Kavane A, Sharma A, Geetha KA, Samantaray S, Maiti S (2018) Molecular marker analysis of genetic diversity in relation to reproductive behavior of *Commiphora wightii* population distributed in Gujarat and Rajasthan states of India. S Afr J Bot 117:141–148

Booth TH (2017) Assessing species climatic requirements beyond the realized niche: some lessons mainly from tree species distribution modelling. Clim Change 145:259–271

Brindavanam NB, Goraya GS, Singh SP, Kumar A, Tiwari A, Sarvepalli BN, Raturi PP (2022) Genetic diversity in *Commiphora wightii* (Arn.) Bhandari (Guggul): an assessment of populations in conservation sites of kachchh region (Gujarat) of India. Pharmacognosy J 14(4):379–387

Brown JL, Anderson B (2014) Sdmtoolbox: a python–based GIS toolkit for landscape genetic, biogeographic and species distribution model analyses. Methods in Ecol Eval 5:694–700

Brown JL, Bennett JR, French CM (2017) Sdmtoolbox 2.0: the next generation python-based GIS toolkit for landscape genetic, biogeographic and species distribution model analyses. PeerJ 5:e4095

Buechling A, Tobalske C (2010) Predictive habitat modeling of rare plant species in Pacific Northwest forests. West J Appl Forest Res 26(2):71–81

Chen Q, Yin Y, Zhao R, Yang Y, Teixeira da Silva JA, Yu X (2020) Incorporating local adaptation into species distribution modeling of *Paeonia mairei*, an endemic plant to China. Front Plant Sci 10:1717. https://doi.org/10.3389/fpls.2019.01717

Choudhary M, Bano S, Tomar UK (2021) Biannual seed yield, viability and germination in *Commiphora wightii* (Arnott) Bhandari. Biol Life Sci Forum. https://doi.org/10.3390/IECPS2020-08889

Cihal L, Kalab O (2017) Species distribution models for critically endangered liverworts (Bryophyta) from the Czech Republic: a guide to future survey expeditions. Acta Mus Siles Sci Natur 66:101–110

Coban HO, Orucu OK, Arslan ES (2020) MaxEnt modelling for predicting the current and future potential geographical distribution of *Quercus libani* Olivier. Sustainability 12:2671. https://doi.org/10.3390/su12072671

Dauby G, Stevart T, Droissart V, Cosiaux A, Deblauwe V, Simo-Droissart M, Sosef MSM, Porter P, George E, Gereau RE, Couvreur TLP (2017) ConR: an R package to assist large-scale multispecies preliminary conservation assessments using distribution data. Ecol Eval 7(24):11291–11303

De Queiroz TF, Baughman C, Baughman O, Gara M, Williams N (2012) Species distribution modeling for conservation of rare, edaphic endemic plants in White River Valley. Nevada Nat Areas J 32(2):149–158

Dixit AM, Rao SVS (2000) Observation on distribution and habitat characteristics of guggul (*Commiphora wightii*) in the arid region of Kachchh, Gujarat, India. Trop Ecol 41(1):81–88

Elith J, Graham CH, Anderson RP, Dudik M, Ferrier S, Guisan A, Hijmans RJ, Huettmann F, Leathwick JR, Lehmann A, Li J, Lohmann LG, Loiselle BA, Manion G, Moritz C, Nakamura M, Nakazawa Y, Overton JM, Peterson AT, Phillips SJ, Richardson K, Scachetti-Pereira R, Schapire RE, Soberon J, Williams S, Wisz MS, Zimmermann NE (2006) Novel methods improve prediction of species' distributions from occurrence data. Ecography 29:129–151

Elith J, Phillips SJ, Hastie T, Dudík M, Chee YE, Yates CJ (2011) A statistical explanation of MaxEnt for ecologists. Divers Distrib 17:43–57. https://doi.org/10.1111/j.1472-4642.2010.00725.x

Fischer G, Nachtergaele F, Prieler S, van Velthuizen HT, Verelst L, Wiberg D (2008) Global Agro-ecological Zones Assessment for Agriculture (GAEZ 2008). IIASA, FAO, Luxemburg, Rome

Flory AR, Kumar S, Stohlgren TJ, Cryan PM (2012) Environmental conditions associated with bat white nose syndrome mortality in the north-eastern United States. J Appl Ecol 49:680–689

Franklin J (2009) Mapping species distributions: spatial inference and prediction. Cambridge University Press, Cambridge

Gaur A, Singhal H, Tomar UK (2017) Asexual morphological differences in male and female plants of *Commiphora wightii* (Arn.) Bhandari—an endangered medicinal plant. Res Plant Sci 5(2):51–59. https://doi.org/10.12691/plant-5-2-1

Gogol-Prokurat M (2011) Predicting habitat suitability for rare plants at local spatial scales using a species distribution model. Ecol App 21(1):33–47

Goncalves E, Herrera I, Duarte M, Bustamante RO, Lampo M, Velásquez G, Sharma GP, García-Rangel S (2014) Global invasion of *Lantana camara*: has the climatic niche been conserved across continents? PLoS ONE 9(10):111468

Gonzalez-Moreno P, Diez JM, Richardson DM, Vilà M (2015) Beyond climate: disturbance niche shifts in invasive species. Glob Ecol Biogeogr 24:360–370

Guillera-Arroita G, Lahoz-Monfort JJ, Elith J, Gordon A, Kujala H, Lentini PE, McCarthy MA, Tingley R, Wintle BA (2015) Is my specie distribution model fit for purpose? Matching data and models to applications. Glob Ecol Biogeogr 24(3):276–292
Gupta PK, Shivanna R, Mohan Ram HY (1996) Apomixis and polyembryony in the guggul plant, *Commiphora wightii*. Ann Bot 78(1):67–72. https://doi.org/10.1006/anbo.1996.0097
Gupta R, Sharma LK, Rajkumar M, Mohammad N, Khan ML (2023) Predicting habitat suitability of *Litsea glutinosa*: a declining tree species, under the current and future climate change scenarios in India. Landsc Ecol Eng. https://doi.org/10.1007/s11355-023-00537-x
Hamid M, Khuroo AA, Charles B, Ahmad R, Singh CP, Arvid NA (2019) Impact of climate change on the distribution range and niche dynamics of Himalayan birch, a typical tree line species in Himalayas. Biodiver Conserv 28:2345–2370. https://doi.org/10.1007/s10531-018-1641-8
Haque I, Bandopadhyay R, Mukhopadhyay K (2009) Population genetic structure of the endangered and endemic medicinal plant *Commiphora wightii*. Mol Biol Rep 37:847–854. https://doi.org/10.1007/s11033-009-9661-9
Harish Gupta AK, Phulwaria M, Rai MK, Shekhawat NS (2014) Conservation genetics of endangered medicinal plant *Commiphora wightii* in India Thar Desert. Gene 535(2):266–272
Hijmans RJ, Cameron SE, Parra JL, Jones PG, Jarvis A (2005) Very high-resolution interpolated climate surfaces for global land areas. Int J Climatol 25:1965–1978. https://doi.org/10.1002/joc.1276
Holscher B (2011) *Commiphora* Jacq. http://www.plantzafrica.com/plantcd/commiphora.htm—a part of the South African National Biodiversity Institute's plant information website. www.plantzafrica.com.
Horandl E, Cosendai AC, Temsch EM (2018) Understanding the geographic distribution of apomictic plants: a case for a pluralistic approach. Plant Ecol Divers 1:309–320
IUCN (2010) Red List of Threatened Species. www.iucnredlist.org/apps/redlist/details/31231 IUCN, Gland, Switzerland
IUCN Standards and Petitions Subcommittee (2014) Guidelines for using the IUCN red list categories and criteria THE IUCN RED LIST OF THREATENED SPECIES™
Jain N, Nadgauda RS (2013) *Commiphora wightii* (Arnott) Bhandari–A natural source of Guggulsterone: facing a high risk of extinction in its natural habitat. Am J Plant Sci 4(6):57–68
Jindal SK, Singh DV, Moharana PC, Waris A (2009) Annual Report of ICAR. Central Arid Zone Research Institute, Jodhpur, Rajasthan, India, P 152
Jindal SK, Singh DV, Moharana PC, Waris A (2010) Annual Report of ICAR. Central Arid Zone Research Institute, Jodhpur, Rajasthan, India, P 155
Wan JZ, Wang CJ, Tan JF, Yu FH (2017) Climatic niche divergence and habitat suitability of eight alien invasive weeds in China under climate change. Ecol Evol 7:1541–1552
Kaky E, Gilbert F (2019) Assessment of the extinction risks of medicinal plants in Egypt under climate change by integrating species distribution models and IUCN Red List criteria. J Arid Environ 170:103988. https://doi.org/10.1016/j.jaridenv.2019.05.016
Kala CP, Dhyani PP, Sajwan BS (2006) Developing the medicinal plants sector in northern India: challenges and opportunities. J Ethnobiol Ethnomed 2:1–15
Kasera PK, Prakash J (2005) Ecology and cultivation practices of guggul (*Commiphora wightii*): an endangered medicinal plant of the Thar desert in India. In: Majumadar DK, Govil JN, Singh VK, Shar-ma RK, eds Recent Progress in Medicinal Plants, Vol. 9— Plant Bioactive in Traditional Medicine, Stadium Press LLC, Houston, pp 403–423
Kass JM, Vilela B, Aiello-Lammens ME, Muscarella R, Merow C, Anderson RP (2018) *Wallace*: a flexible platform for reproducible modeling of species niches and distributions built for community expansion. Methods Ecol Evol 9:1151–1156. https://doi.org/10.1111/2041-210X.12945
Kass JM, Meenan SI, Tinoco N, Burneo SF, Anderson RP (2021) Improving area of occupancy estimates for parapatric species using distribution models and support vector machines. Ecol Appl 31(1):1–15
Khan AM, Li Q, Saqib Z, Khan N, Habib T, Khalid N, Majeed M, Tariq A (2022) MaxEnt modelling and impact of climate change on habitat suitability variations of economically important Chilgoza Pine (*Pinus gerardiana* Wall.) in South Asia. Forests 13:715. https://doi.org/10.3390/f13050715
Kulhari A, Sheorayan A, Kalia S, Chaudhury A, Kalia RK (2012) Problems, progress and future prospects of improvement of *Commiphora wightii* (Arn.) Bhandari, an endangered herbal magic, through modern biotechnological tools: a review. Genet Resour Crop Eval 59:1223–1254
Kulhari A, Sheorayan A, Singh R, Dhawan AK, Kalia RK (2014) Survey, collection and conservation of *Commiphora wightii* (Arn.) Bhandari–an important medicinal plants heading towards extinction. Indian For 140(12):1171–1183
Kulloli RN, Mathur M, Kumar S (2016) Dynamics of top-down factors with relation to ecological attributes of an endangered species *Commiphora wightii*. J Appl Nat Sci 8(3):1556–1564
Kumar S, Kulloli RK (2017) Effect of associated species on distribution of *Commiphora wightii* in Indian arid zone. Taiwania 62(1):43–49
Kumar S, Mathur M (2014) Impact of invasion by *Prosopis juliflora* on plant communities in arid grazing lands. Trop Ecol 55(1):33–47
Kumar S, Shanker V (1982) Medicinal plants of Indian desert: *Commiphora wightii* (Arn.) Bhandari. J Arid Environ 5:1–11
Kumar S, Stohlgren TJ (2009) MaxEnt modelling for predicting suitable habitat for threatened and endangered tree *Canacomyrica monticola* in New Caledonia. J Ecol Nat Environ 1:94–98
Kumar S, Stohlgren TJ, Chong GW (2006) Spatial heterogeneity influences native and non-native plant species richness. Ecology 87:3186–3199
Lal H, Kasera PK (2010) Status and distribution range of guggal: a critically endangered medicinal plant from the Indian Thar Desert. Sci Cult 76:11–12
Li Y, Li M, Li C, Liu Z (2020) Optimized maxent model predictions of climate change impacts on the suitable distribution of *Cunninghamia lanceolata* in China. Forests 11:302. https://doi.org/10.3390/f11030302
Ma B, Sun J (2018) Predicting the distribution of *Stipa purpurea* across the Tibetan Plateau via MaxEnt model. BMC Ecol 18:10. https://doi.org/10.1186/s12898-018-0165-0
Maheshwari DV (2010) Guggul plantation shows good success in Kutch. Find Articles/Business/DNA: Daily News and Analysis, Mumbai
Mall RK, Sonkar G, Sharma NK, Singh N (2016). Impacts of climate change on agriculture sector in Madhya Pradesh—an Assessment Report. https://doi.org/10.13140/RG.2.1.3010.0247
Marcer A, Sáez L, Molowny-Horas R, Pons X, Pino J (2013) Using species distribution modelling to disentangle realized versus potential distributions for rare species conservation. Biol Conserv 166:221–230. https://doi.org/10.1016/j.biocon.2013.07.001
Marco P, Villen S, Mendes P, Noberga C, Cortes L, Castro T, Souza R (2018) Vulnerability of cerrado threatened mammals: an integrative landscape and climate modeling approach. Biodiver Conser 29:1637–1658. https://doi.org/10.1007/s10531-018-1615-x
Mathur M (2014a) Does adaptive strategy for delayed seed dispersal affect extinction probability of a desert species? An assessment using the population viability analysis and glass house experiment. Brazil Arc Biol Techno 57(5):774–781. https://doi.org/10.1590/S1516-8913201402407
Mathur M (2014b) Spatio-temporal variability in distribution patterns of *Tribulus terrestris*: linking patterns and processes. J Agri Sci Technol 16:1187–1201
Mathur P, Mathur M (2023) Machine learning ensemble species distribution modeling of an endangered arid land tree *Tecomella undulata*: a global appraisal. Arab J Geosci 16:131. https://doi.org/10.1007/s12517-023-11229-z
Mathur M, Sundarmoorthy S (2013) Inter-specific association of herbaceous vegetation in semi-arid Thar desert. India Range Manag Agrofor 34(1):26–32
Mathur M, Sundaramoorthy S (2019) Woody perennial diversity at various land forms of the five agro-climatic zones of Rajasthan, India. In: Ramawat K (ed) Biodiversity and Chemotaxonomy. Sustainable Development and Biodiversity, vol 24. Springer, Cham. https://doi.org/10.1007/978-3-030-30746-2_5
McCune JL, Rosner-Katz H, Bennett JR, Schuster R, Kharouba HM (2020) Do traits of plant species predict the efficacy of species distribution models for finding new occurrences? Ecol Evol 10:1–14
Mcsweeney CF, Jones RG, Lee RW, Rowell DP (2015) Selecting CMIP5 GCMS for downscaling over multiple regions. Clim Dynam 44:3237–3260
Meinshausen M, Nicholls ZRJ, Lewis J, Gidden MJ, Vogel E, Freund M, Beyerle U, Nauelsd A, Bauer N, Canadell JG, Daniel JS, John A, Krummel PB, Luderer G, Meinshausen N, Montzka SA, Rayner PJ, Reimann S, Smith SJ, Berg MVD, Velders GJM, Vollmer MK, Wang RHJ (2020) The shared socioeconomic pathway (SSP) greenhouse gas concentration and their

extension to 2500. Geosci Model Dev 13:3571–3605. https://doi.org/10.5194/gmd-13-3571-2020
Mertia RS, Sinha NK, Kandpal BK, Singh D (2010) Evaluation of Indian Myrrh (*Commiphora wightii*) landraces for hyper arid Thar Desert. Indian J Agric Sci 80(10):869–871
Millennium Ecosystem Assessment (2005) Ecosystems and human well-being: global assessment reports. Island Press, Washington DC
Mishra SN, Kumar D, Kumar B, Tiwari S (2021) Assessing impact of varying climatic conditions on distribution of *Buchanania cochinchinensis* in Jharkhand using species distribution modelling approach. Curr Res Environ Sustain 3:100025. https://doi.org/10.1016/j.crsust.2021.100025
Mondal T, Bhatt D, Ramesh K (2022) Bioclimatic modelling of *Lantana camara* invasion in the Shivalik landscape of Western Himalaya. Trop Ecol. https://doi.org/10.1007/s42965-022-00264-8
Mousazade M, Ghanbarian G, Pourghasemi HR, Safaeian R, Cerda A (2019) Maxent data mining technique and its comparison with a bivariate statistical model for predicting the potential distribution of *Astragalus fasciculifolius* Boiss. Sustainability 11:3452. https://doi.org/10.3390/su11123452
Nunez-Penichet C, Cobos ME, Soberon J (2021) Non-overlapping climatic niches and biogeographic barriers explain disjunct distributions of continental *Urania* moths. Fron Biogeo 13(2):e52142
Osorio-Olivera L, Lira-Noriega A, Soberon J, Townsend PA, Facon M, Contreas Diaz RG, Martinez-Meyer E, Barve V, Barve N (2020) Ntbox: an R package with graphical user interface for modelling and evaluating multidimensional ecological niches. Methods Ecol Evol 11:1199–1206. https://doi.org/10.1111/2041-210X.13452
Padalia H, Srivastava V, Kushwaha SPS (2014) Modelling potential invasion range of alien invasion species, *Hyptis suaveolens* (L) in India: comparison of MaxEnt and GARP. Ecol Infor 22:36–43
Parmar PJ (2003) Loss of *Commiphora wightii* (Arn.) Bhandari in Indian Desert. Bull Bo Surv India 45:77–90
Pecchi M, Marchi M, Burton V, Giannetti F, Moriondo M, Bernetti I, Bindi M, Chirici G (2019) Species distribution modelling to support forest management. A literature review. Ecol Modell 411:108817
Phillips SJ, Dudik M (2008) Modelling of species distributions with Maxent: new extensions and a comprehensive evaluation. Ecography 31:161–175
Phillips SJ, Anderson RP, Schapire RE (2006) Maximum entropy modeling of species geographic distributions. Ecol Model 190:231–259
Pradhan P (2016) Strengthening Maxent modelling through screening of redundant explanatory bioclimatic variables with variance inflation factor analysis. Researcher 8(5):29–34
Prakash J, Kasera PK, Chawan DD (2000) A report on polyembryony in *Commiphora wightii* from Thar Desert, India. Curr Sci 78(10):1185–1187
Priti H, Aravind NA, Uma Shaanker R, Ravikanth G (2016) Modelling impacts of future climate on the distribution of Myristicaceae species in the Western Ghats, India. Ecol Eng 89:14–23
Purohit S, Rawat N (2022) MaxEnt modeling to predict the current and future distribution of *Clerodendrum infortunatum* L. under climate change scenarios in Dehradun district, India. Model Earth Syst Environ 8:2051–2063. https://doi.org/10.1007/s40808-021-01205-5
Radosavljevic A, Anderson RP (2014) Making better Maxent models of species distributions: complexity, overfitting and evaluation. J Biogeogr 41:629
Rahaman SM, Ghosh BG, Garai S, Khatun M, Ranjan A, Mishra R, Tiwari S (2022) Assessing potential distribution zone prone to invasion risk of *Hyptis suaveolens* (L) in Jharkhand, Eastern India using MaxEnt. Int J Ecol Environ Sci 48:281–294
Rajpoot R, Adhikari D, Verma S, Saikia P, Kumar A, Grant KR, Dayanandan A, Kumar A, Khare PK, Khan ML (2020) Climate models predict a divergent future for the medicinal tree *Boswellia serrata* Roxb. in India. Glob Ecol Conserv 23:e01040
Ramawat KG, Mathur M, Dass S, Suthar S (2008) Guggulsterone: a potent natural hypolipidemic agent from *Commiphora wightii*—problems, perseverance, and prospects In: Ramawat KG, Merillon JM eds Bioactive Molecules and Medicinal Plants. Springer, Heidelberg: 101–121. https://doi.org/10.1007/978-3-540-74603-4_5
Ray D, Behera MD, Jacob J (2014) Indian Brahmaputra valley offers significant potential for cultivation of rubber tree. Curr Sci 107(3):461–469
Ray D, Behera MD, Jacob J (2018) Evaluating ecological niche models: a comparison between Maxent and GARP for predicting distribution of *Hevea brasiliensis* in India. Proc Natl Acad Sci India Sect B Biol Sci 88:1337–1343
Reddy CS, Meena SL, Krishna PH, Charan PD, Sharma KC (2012) Conservation threat assessment of *Commiphora wightii* (Arn.) Bhandari—an economically important species. Taiwania 57(3):288–293
Remya K, Ramachandran A, Jayakumar S (2015) Predicting the current and future suitable habitat distribution of *Myristica dactyloides* Gaertn. using Maxent model in the Eastern Ghats, India. Ecol Eng 82:184–188
Renner IW, Warton DI (2013) Equivalence of MAXENT and Poisson point process models for species distribution modeling in ecology. Biometrics 69:274–281
Rong Z, Zhao C, Liu J, Gao Y, Zang F, Guo Z, Mao Y, Wang L (2019) Modeling the effect of climate change on the potential distribution of Qinghai Spruce (*Picea crassifolia* Kom.) in Qilian mountains. Forest 10:62. https://doi.org/10.3390/f10010062
Saini LS, Rajput SK, Rathor TR, Tomar UK (2018) Non-destructive harvesting of oleo-gum resin in *Commiphora wightii* (Arnott) Bhandari–a critically endangered plant. Ind Crops Prod 113:259–265
Salam N, Reshi ZA, Shah MA (2018) Habitat suitability modeling for *Lagotis cashmeriana* (Royle) Ruprr., a threatened species endemic to Kashmir Himalayan alpines. Geol Ecol Landsc. https://doi.org/10.1080/24749508.2020.1816871
Samanta JA, Saravanan R, Gajbhiye NA, Mandal K (2012) Impact of soil moisture levels on growth, photosynthetic competence and oleo–gum–resin production of guggal (*Commiphora wightii*). J Trop For Sci 24(4):538–545
Samanta JN, Mandal K, Saravanan R, Gajbhiye N, Velumani R (2016) Influence of tapping position, intensity of tapping and season on gummosis of guggal (*Commiphora wightii*), oleo-gum-resin yield and quality. Ind J Ag Sci 86(1):144–146
Sarikaya O, Karaceylan IB, Sen I (2018) Maximum entropy modelling (Maxent) of current and future distributions of *Ips mannsfeldi* (Wachtl, 1879) (Curculionidae: Scolytinae) in Turkey. App Ecol Environ Res 16:2527–2535
Sarma B, Baruah PS, Tanti (2018) Habitat distribution modelling for reintroduction and conservation of *Aristolochia indica* L.—a threatened medicinal plant in Assam, India. J Threat Taxa 10(11):12531–12537. https://doi.org/10.11609/jott.3600.10.11.12531-12537
Sen S, Ameya G, Srirama R, Ravikanth G, Aravind NA (2016a) Modeling the impact of climate change on wild *Piper nigrum* (Black Pepper) in Western Ghats, India using Ecological Niche models. J Plant Res 129:1033–1040
Sen S, Shivaprakash KN, Aravind NA, Ravikanth G, Dayanandan S (2016b) Ecological niche modeling for conservation planning of an endemic snail in the verge of becoming a pest in cardamom plantations in the Western Ghats Biodiversity Hotspot. Ecol Evol 6:6510–6523
Sharma S, Arunachalam K, Bhavsar D, Kala R (2018) Modeling habitat suitability of *Perilla frutescens* with Maxent in Uttarakhand—a conservation approach. J Appl Res Med Aromatic Plants 10:99–105
Sillero N, Barbosa AM (2021) Common mistakes in ecological niche models. Int J Geogr Infor Sci 35(2):213–226. https://doi.org/10.1080/13658816.2020.1798968
Singh V, Singh M (2006) Biodiversity of Desert National Park, Rajasthan. Botanical Survey of India, Kolkata, p 344
Singhal H, Gaur A, Tomar UK (2014) Observations on flowering and fruiting in *Commiphora wightii* (Arnott) Bhandari. Eur J Med Plants 4(9):1087–1097
Sinha NK, Mertia RS, Kandpal BK, Kumawat RN, Santra P, Daleep S (2012) Morphological characterization of guggal (*Commiphora wightii*) provenances from extremely arid parts of India. For Trees Livelihoods 21(1):63–69. https://doi.org/10.1080/14728028.2012.669579
Soni V (2010) In-situ conservation of *Commiphora wightii* a red-listed medicinal plant species of Rajasthan state, India. Project Report, Species Survival Commission and IUCN 1–30.
Thakur KK, Bhat P, Kumar A, Ravikanth G, Saiki P (2022) Distribution mapping of *Bauhinia vahlii* Wight & Arn. in India using ecological niche modelling. Trop Ecol 63:286–299. https://doi.org/10.1007/s42965-021-00197-8
Tiwari S, Mishra SN, Kumar D, Kumar B, Vaidy SN, Ghosh BG, Rahaman SM, Khatun M, Garai S, Kumar A (2022) Modelling the potential risk zone of *Lantana camara* invasion and response to climate change in eastern India. Ecol Process 11:10. https://doi.org/10.1186/s13717-021-00354-w

Tomar UK, Singhal H, Gaur A, Saini LS (2021) Population density, genetic diversity and hot spots of *Commiphora wightii* (Arnott) Bhandari in Rajasthan State. J Appl Res Med Aromatic Plants 25:100323. https://doi.org/10.1016/j.jarmap.2021.100323

Tomar UK (2013) Assessment of Guggul germplasm for studying population density, diversity, female-male plant's ratio for in situ and ex situ conservation in Rajasthan. SFD Rajasthan. ICFRE Report. https://forest.rajasthan.gov.in/content/dam/raj/forest/ForestDepartment/PDFs/Department%20Wing/Forest%20Research/Silva%20Technical%20Publication/PROGRESS%20REPORT%20OF%20THE%20PROJECT%20BY%20AFRI/Final_Progress_Report_March_2014_Guggal.pdf

Tripathi A, Shukla JK, Gehlot A, Mishra DK (2016) Condensed node proliferation technique (CNPT): a better low-cost macro-propagation approach through min-cuttings of *Commiphora wightii* (Arn.) Bhandari an endangered plant of Indian Thar Desert. Adv For Sci 3(4):65–69

Tuanmu MN, Jetz W (2015) A global, remote sensing based characterization of terrestrial habitat heterogeneity for biodiversity and ecosystem modelling. Global Ecol Biogeogr 24:1329–1339. https://doi.org/10.1111/geb.12365

Ved D, Saha D, Ravikumar K, Haridasan K (2015) *Commiphora wightii*. The IUCN Red List of Threatened Species. https://doi.org/10.2305/IUCN.UK.2015-2.RLTS.T31231A50131117.en.e.T31231A50131117

Verma RK, Ibrahim M, Fursule A, Mitra R, Sastry JLN, Ahmad S (2022) Metabolomic profiling of *Commiphora wightii* (Arn.) Bhandari bark oleogum-resin, and stem collected from different geographical regions of India. S Afr J Bot 149:211–221

Vitor HFG, Stephanie DI, Niels R et al (2018) Species Distribution Modelling: contrasting presence-only models with plot abundance data. Sci Rep 8:1003. https://doi.org/10.1038/s41598-017-18927-1

Wang HH, Wonkka CL, Treglia ML, Grant WE, Smeins FE, Rogers WE (2015) Species distribution modelling for conservation of an endangered endemic orchid. AoB Plants 7:e039. https://doi.org/10.1093/aobpla/plv039

Warren DL, Glor RE, Turelli M (2010) ENMTools: a toolbox for comparative studies of environmental niche models. Ecography 33:607–611

Wei BO, Wang R, Hou K, Wang X, Wu W (2018) Predicting the current and future cultivation regions of *Carthamus tinctorius* L. using Maxent model under climate change in China. Glob Ecol Conser 16:e00477. https://doi.org/10.1016/j.gecco.2018.e00477

West AM, Kumar S, Brown CS, Stohlgren TJ, Bromberg J (2016) Filed validation of an invasive species maxent model. Ecol Infor 36:126–134

Wisz MS, Hijmans RJ, Li J, Peterson AT, Graham CH, Guisan A (2008) Predicting species distributions working group. Effects of sample size on the performance of species distribution models. Diver Distri 14:763–773

Wu J, Xia C, Meier J, Li S, Hu X, Lala DS (2002) The hypolipidemic natural product guggulsterone acts as an antagonist of the bile acid receptor. Mol Endocrinol 16(7):1590–1597. https://doi.org/10.1210/mend.16.7.0894

Xu W, Jin J, Cheng J (2021) Predicting the potential geographic distribution and habitat suitability of two economic forest trees on the Loess Plateau, China. Forests 12:747. https://doi.org/10.3390/f12060747

Yadava BBL (2011) *Commiphora wightii* (Gum-Guggul) present status in India: an overview. Herbal Tech Industry 8(1):24–28

Yadava BBL, Billore KV, Joseph JG, Chaturvedy DD (1999) Cultivation of GUGGULU," Central Council in Ayurveda and Siddha (Ayush), New Delhi, 1–87.

Ye XZ, Zhao GH, Zhang MZ, Vui XY, Fan HH, Liu B (2020) Distribution pattern of endangered plants *Semiliquidambar catayensis* (Hamamelidaceae) in response to climate change after the last interglacial period. Forest 11:434. https://doi.org/10.3390/f11040434

Yi YJ, Cheng X, Yang ZF, Zhang SH (2016) Maxent modeling for predicting the potential distribution of endangered medicinal plant (*H. riparia* Lour) in Yunnan, China. Ecol Eng 92:260–269

Zhang Y, Tang J, Ren G, Zhao K, Wang X (2021) Global potential distribution prediction of *Xanthium italicum* based on Maxent model. Sci Rep 11:16545. https://doi.org/10.1038/s41598-021-96041-z

Zhao G, Cui X, Sun J, Li T, Wang Q, Ye X, Fan B (2021) Analysis of the distribution pattern of Chinese *Ziziphus jujuba* under climate change based on optimized biomod2 and MaxEnt models. Ecol Indic 132:108256. https://doi.org/10.1016/j.ecolind.2021.108256

Publisher's Note